Quantification of the Effect of Bridge Pier Encasement on Headwater Elevation Using HEC-RAS

by

Abhijit Sharma Subedi

Submitted in Partial Fulfillment of the Requirements

for the Degree of

Master of Science in Engineering

in the

Civil and Environmental Engineering Program

YOUNGSTOWN STATE UNIVERSITY

June 2017

Quantification of the Effect of Bridge Pier Encasement on Headwater Elevation Using HEC-RAS

Abhijit Sharma Subedi

Signature:

Abhijit Sharma Subedi, Student — Date

Approvals:

Suresh Sharma, Thesis Advisor — Date

Anwarul Islam, Committee Member — Date

Tony Vercellino, Committee Member — Date

Dr. Salvatore A. Sanders, Dean of Graduate Studies — Date

ABSTRACT

Bridges are one of the most expensive and vital infrastructures in the transportation system. However, the bridge substructure such as piers, undergoes various kinds of deterioration and damages overtime. Different kinds of repair and rehabilitation practices are needed to protect bridges from future damages. One of such common methods of pier protection is pier encasement. Pier encasement involves enclosing an existing pier with suitable materials such as PVC pipe, to increase its strength. However, the process of pier encasement increases the overall width of the pier, which might result in the rise of headwater elevation at the bridge vicinity. Moreover, this rise in headwater elevation may cause serious problems in areas located in high-risk flood zones. When the bridge and its piers are located within the defined floodway boundaries of a Federal Emergency Management Administration (FEMA) National Flood Insurance Program (NFIP) Zone AE, no rise in water surface elevation must be maintained. Therefore, this study was undertaken to find the effects of pier encasement on headwater elevation under varying pier and channel configurations. In order to study the impact of pier encasement, HEC-RAS, was used for hydraulic simulation. The hydraulic simulation was carried out for various channel configurations. The comparison was done for encased and non-encased pier conditions for the varying conditions of channel configurations, such as channel width, slope, and flow volume. The study showed the rise in headwater elevation for the channel with a smaller bottom width (20 ft, 40 ft, 60 ft, and 80 ft). The rise in headwater elevation was further increased for steeper slopes (0.7% and 1.0%) and for higher flow volume.

Furthermore, winter ice jam around a bridge structure can cause serious damage to the bridge and has been one of the major problems with bridges in the northern belt of the

USA. The bridge piers, which comes in contact with ice, has a significant impact on ice jam. Moreover, a bridge pier enforces substantial changes in river flow dynamics, especially in ice jam conditions. Therefore, the effect of pier encasement on water surface elevation during the winter period (ice jam) was also analyzed using HEC-RAS. After running numerous models with various channel configurations, it was found that the pier encasement effect was minimal in head water elevation even for the ice jammed bridges. Nevertheless, the minor rise was noticed for smaller channel bottom widths (20 ft and 40 ft) only with steeper slope (0.7% and 1.0%).

Since these findings were derived using various hypothetical channel configurations, the further application of this study was pursued in various existing bridges in the Grand River, OH, to verify that the concept derived from the generic channel section is valid in real word applications. The pier encasement was done for bridges located on the Grand River. The hydraulic simulation was conducted for computing water surface elevation for both encased and non-encased bridge structures. The result was found to be consistent with the parametric study performed for generic channel sections. After encasement, the wider channel showed no rise in water surface elevation, however, the channel with smaller bottom width showed a slight rise in water surface elevation (0.03 ft).

ACKNOWLEDGEMENTS

My gratitude goes to my thesis advisor, Dr. Suresh Sharma, for his unwavering support, encouragement, and mentorship throughout this research. I am also deeply grateful to the Department Chair, Dr. Anwarul Islam, for his wonderful guidance and suggestions to accomplish this research. I am highly indebted to my thesis committee member, Dr. Tony Vercellino for his willingness to serve on my thesis committee and providing me with valuable suggestions and feedbacks.

I would like to acknowledge Ohio Department of Transportation for providing grant support to conduct this research. I would also like to extend my earnest thanks to Thomas K. Birnbrich, Ohio Department of Transportation, who provided the necessary research data and guidelines for this study.

I am very much thankful to Ms. Linda Adovasio for her support and assistance at YSU. I am immensely grateful to all of my friends, who helped and encouraged me at various stages during the research works and thesis writing. In addition, I am much indebted to Niraj Lamichhane for providing ideas and suggestions while conducting this study.

Lastly, I am highly obliged, especially to my father Rajendra Sharma Subedi and my mother Anjana Sharma, for all the love, inspiration and motivation, which have been the greatest gift anyone has ever given to me. I am also thankful to my siblings Shradha Sharma, Sandhya Sharma and Suraj Subedi, who made me realize my own potential, supported and encouraged me to complete this research. Last but not the least, I would like to thank my cousin, Sushma Subedi living in Pittsburg, for the love, support and comfort she provided me in this foreign land.

Table of Contents

ABSTRACT ii

ACKNOWLEDGEMENTS iv

LIST OF FIGURES vi

LIST OF TABLES viii

List of Abbreviations ix

Chapter I. Introduction 1

Chapter 2. Quantification of the Effect of Bridge Pier Encasement on Headwater Elevation Using HEC-RAS 8

Chapter 3. Pier Encasement Effect on Headwater Elevation due to Winter Ice Cover and Ice Jam 42

Chapter 4. Effect of Pier Encasement on Headwater Elevation in Grand River Using HEC-RAS Model 66

Chapter 5. Conclusions and Recommendations 73

LIST OF FIGURES

Figure 2-1: H-Pile- a) pier before encasement and b) pier after encasement 29

Figure 2-2: Channel profile and cross section locations.. 29

Figure 2-3: Channel cross-section in HEC-RAS with 180 ft bottom width. 30

Figure 2-4: Bridge cross-section with pier location in the channel with 180 ft bottom width. 30

Figure 2-5: Profile plot for 20 ft channel bottom width of 1% channel slope with existing pier. 31

Figure 2-6: Profile plot for 20 ft channel bottom width of 1% channel slope with proposed pier.. 31

Figure 2-7: The difference in WSE at most upstream for 20 ft channel section. 32

Figure 2-8: The difference in WSE at immediate upstream for 20 ft channel section. 32

Figure 2-9: The difference in WSE at most upstream for 100 ft channel section. 33

Figure 2-10: The difference in WSE at immediate upstream for 100 ft channel section. 33

Figure 2-11: The difference in WSE at most upstream for 180 ft channel section. 34

Figure 2-12: The difference in WSE at immediate for 180 ft channel section 34

Figure 2- 13: The difference in WSE with respect to change in area 35

Figure 3-1: The difference in WSE at most upstream for 20 ft channel section. 58

Figure 3-2: The difference in WSE at immediate upstream for 20 ft channel section. 58

Figure 3-3: The difference in WSE at most upstream for 100 ft channel........................ 59

Figure 3-4: The difference in WSE at immediate upstream for 100 ft channel section. .. 59

Figure 3-5: The difference in WSE at most upstream for 180 ft channel section. 60

Figure 3-6: The difference in WSE at immediate for 180 ft channel section.................. 60

Figure 4-1: Hydraulic model of Grand River in HEC-RAS with bridge station number. 70

Figure 4-2: The difference in water surface elevation at bridge upstream before and after pier encasement for various bridge stations. 70

LIST OF TABLES

Table 2-1: Typical drag coefficients for various pier shapes 36

Table 2-2: Pile pier and encasement data provided by ODOT 36

Table 2-3: Reach length and location from the centerline of the bridge. 36

Table 2-4: Allowable state surcharge limits as of 2003 (Gary et al., 2003) 37

Table 2-5: No-rise condition for the circular pier. 38

Table 2-6: No-rise condition for the square pier. 40

Table 3-1: c values for different conditions taken from USACE, 2002 61

Table 3-2: HEC-RAS default ice jam parameters 61

Table 3-3: No-rise condition for the circular pier. 62

Table 3-4: No-rise condition for the square pier. 64

Table 4-1: The difference in water surface elevation before and after the pier encasement at bridge upstream 71

LIST OF ABBREVIATIONS

AASHTO	American Association of State Highway and Transportation
AFDD	Accumulated Freezing Degree Days
FEMA	Flood Emergency Management Agency
HEC-RAS	Hydraulic Engineering Center River Analysis System
LiDAR	Light Detection and Ranging
NCDC	National Climatic Data Center
NFIP	National Flood Insurance Program
NOAA	National Oceanic and Atmospheric Administration
NWS	National Weather Service
ODOT	Ohio Department of Transportation
PVC	Polyvinyl Chloride
ROC	Research On-call
USD	United States Dollars
USGS	United States Geological Survey
USACE	United States Army Corps of Engineers
USACE-HEC	United States Army Corps of Engineers-Hydrologic Engineering Center
WSE	Water Surface Elevation

Chapter I. Introduction

Bridges are the most important components of the transportation system, which in turn has a substantial effect on the economic development of the nation (Laursen., 1984). However, the deterioration of bridge substructure has become a serious problem across the United States (Steven, 2012). Moreover, the initial design of bridges and their maintenance have constantly been significant challenge for engineers and constructors over time (Brandimarte et al., 2006). Tilly (2011) reported that the majority of bridges require repair within the first 11 to 20 years of their service life. Therefore, a noteworthy portion of the transportation budget is spent on bridge maintenance and rehabilitation. Piers are the integral part of a bridge substructure and generally, the process of pier encasement is undertaken to restore and repair the pier to increase its useable service life. The process of pier encasement increases the pier width and perimeter, which may result in increased water surface elevation at the bridge vicinity. In high-risk flood zones, a rise in headwater elevation can be fatal due to flooding of these low-lying areas.

Flooding has been one of the crucial issues in the United States. In the United States, flooding accounts for the annual average death of 80 people and property loss of approximately 8 billion USD (USGS, 2016). This led to the establishment of National Flood Insurance Program (NFIP) administered by Federal Emergency Management Agency (FEMA), to address the repeated flooding damages. The NFIP requires permitting if any encroachment work is carried out in the floodway. Around 100,000 flood hazard maps, covering 150,000 square miles of floodplain area for 19,200 communities have been already produced by FEMA (NFIP, 2002). FEMA typically considers the bridge pier in a floodway as an encroachment (Charbeneau et al., 2001). Therefore, before any rehabilitation process, it becomes imperative to analyze the effect of pier encasement on headwater elevation. Since the obstruction to flow may increase with pier encasement, it is essential to conduct hydraulic analysis at each structure location and quantify the change in water surface elevation.

Likewise, river ice jam in cold regions of the United States has always been a great matter of concern, especially for the river infrastructures, such as bridges. Ice jam and ice accumulations incur an annual damage of about $120 Million (USD) in the United States (White et al., 2006). The process of an ice jam or accumulation limits the conveyance of channel especially near the bridge site due to the obstruction in the bridge. This reduction in conveyance might lead to an increase in water surface elevation (Sui et al., 2002a). Thus, it might further enhance the backwater effect with an increase in the ice jam thickness particularly due to bridge pier encasement. Especially in bridges, the piers tend to obstruct the passage of ice boosting the frequency and occurrence of ice jam (Beltaos et al., 2006).

The comparison of simulated headwater elevation for encased and non-encased pier condition was studied and analyzed using Hydraulic Engineering Center River Analysis system (HEC-RAS 4.1). For this, a generic hypothetical channel section with varying widths and number of piers were developed in HEC-RAS in order to see the effects of the encasement on a structure with multiple piers. Since such type of analysis should be conducted in various channel configurations, it was practically not feasible to utilize the real world cases, as it required large numbers of channels with several cross section information.

However, in order to verify that the concept derived using hypothetical generic channel section is applicable for all type of real world scenarios, the same concept is utilized for the bridges located in Grand River, OH. The Grand River is one of the biggest river located in the Northeast Ohio.

Scopes and Objectives

Many bridge rehabilitation projects involve a deck replacement with the above-noted pier encasement as an element of the repair. The work within the waterway may be minimal and a detailed hydraulic analysis fully conforming to the process required for development in a FEMA Zone AE can be costly and time-consuming. While determining the rise in surface water elevations for every bridge pier-undergoing repair is very time-consuming and expensive, this project will conduct a parametric study of the effect of pier encasement on the rise of surface water elevations at the vicinity of the bridge by developing a one-dimensional HEC-RAS model. Even though the two-dimensional variation of water surface can be expected immediately upstream of a pier, the water level may not change the width and one-dimensional effect will be dominant farther upstream (Charbeneau & Holley, 2001). More importantly, no research has been published so far to provide detailed information of two-dimensional variation of water surface. In fact, one-dimensional HEC-RAS simulation will be an appropriate choice for water surface profile computation. Understanding of the variation in hydraulics and water surface profile due to increased pier width is not only a crucial issue in bridge design but also in its repair and maintenance.

The main objectives of this research are:

I. To document the effect of pile pier encasement under varying model conditions using HEC-RAS to determine if the water surface elevations can be consistently found to show a no-rise condition so that individual analysis can be avoided;

II. To document the effect of pile pier encasement on water surface elevation due to winter ice cover and ice jams using HEC-RAS model;

III. To test the study in real field scenario for the bridges located at Grand River to determine the changes in headwater elevation for the two scenarios with ice jam and without ice jam.

Methodology for Objective I

a. Create a typical trapezoidal river cross section model in HEC-RAS with multiple cross sections and bridge over it;
b. Incorporate different channel slopes and different bottom channel width into the model;
c. Prepare input discharge data to be supplied to a model in order to simulate a model.
d. Run all the channel and pier configurations for both non-encased and encased conditions;
e. Compare and analyze the water surface elevation for these encased and non-encased models for all the channel bottom width and slopes.

Methodology for Objective II

a. Prepare winter discharge records and ice thickness information;

b. Run all the channel and pier configurations for both non-encased and encased conditions;
c. Compare and analyze the water surface elevation for these encased and non-encased models for all the channel and pier configurations.

Methodology for Objective III

a. Simulate the model for the existing pier condition and record the water surface elevation at bridge upstream in the Grand River;
b. Supply an encasement of two feet to all the pier and run the simulation and record the water surface elevation;
c. Conduct a study for two scenarios with ice jam and without ice jam;
d. Compare and analyze the water surface elevation recorded in both cases.

Thesis structure

This thesis is broadly divided into four chapters. The first chapter discusses background, scope, objectives, and thesis structure. The second chapter evaluates the effects of slope, channel bottom width, the width of the pier and river discharge on water surface elevation in encased and non-encased pier conditions. This chapter also includes the narrative theoretical description, overall modeling approach and model input data, and variables associated with modeling in one-dimensional steady flow using HEC-RAS model.

Chapter 3 discusses the effects of winter ice cover and an ice jam on water surface elevation in encased and non-encased pier conditions. It also evaluates the effects of slope, channel bottom width, and river discharge on water surface elevation after the pier encasement. Chapter 3 also includes the narrative theoretical description, overall modeling approach and model input data associated with ice jam modeling HEC-RAS model.

Chapter 4 discusses the application of the study in real field scenario. It evaluates the change in water surface elevation due to pier encasement on bridges located on the Grand River, OH. The bridge piers located in Grand River were encased and analyzed for two scenarios of ice jam and without ice jam. Finally, Chapter 5 discusses the conclusion of the overall research.

This thesis is written in journal article format. Since each article should stand alone as an independent article, readers may find some redundancy in the following chapters.

Reference

Ainge, Steven W. "Repair and Strengthening of Bridge Substructures." (2012).

Beltaos, Spyros, et al. "Formation of breakup ice jams at bridges." Journal of Hydraulic Engineering 132.11 (2006): 1229-1236.

Brandimarte, Luigia, et al. "Stochastic flow analysis for predicting river scour of cohesive soils." Journal of hydraulic engineering 132.5 (2006): 493-500.

Charbeneau, Randall J., and Edward Raymond Holley. Backwater effects of bridge piers in subcritical flow. Center for Transportation Research, Bureau of Engineering Research, University of Texas at Austin, 2001.

Laursen, Emmett M. "Assessing vulnerability of bridges to floods." Transportation Research Record 950.2 (1984).

Sui, Jueyi, and B. Karney. "Effects of ice on the hydraulics of inner Mongolia Reach of the Yellow River." Proceedings of the IAHR International Symposiums on Ice Problems. Vol. 1. Otago, New Zealand, 2002a.

Tilly, Graham P. "Dynamic behavior and collapses of early suspension bridges." Proceedings of the Institution of Civil Engineers-Bridge Engineering. Vol. 164. No. 2. Thomas Telford Ltd, 2011.

White, Kathleen D., Andrew M. Tuthill, and Linnzi Furman. "Studies of ice jam flooding in the United States." Extreme Hydrological Events: New Concepts for Security. Springer Netherlands, 2006. 255-268.

Chapter 2. Quantification of the Effect of Bridge Pier Encasement on Headwater Elevation Using HEC-RAS

Abstract

The deterioration of bridge substructures has been a serious concern across the United States. Therefore, pier encasement is one of the most common practices to repair and strengthen the bridge substructure. Pier encasement is a process of restoring and reusing the existing pile piers during the repair or replacement of the bridge superstructure, which involves enclosing the existing pier with certain materials like polyethylene or PVC pipe. However, this process of enclosing pier might result in increased water surface elevation due to increase in pier width, which could be very detrimental in high-risk flood zone areas. Furthermore, it may create an adverse impact on the stability of bridge due to scouring action around the bridge pier. Two crucial factors, which can mainly influence the backwater effect, are channel characteristics and flow properties. Therefore, in this research, a widely accepted hydraulic tool, Hydraulic Engineering Center-River Analysis System (HEC-RAS), was used to perform the hydraulic simulation near the bridge sites. The hydraulic simulations were carried out for various channel configuration and pier sizes with a wide range of flows in order to see the effects of pier encasement on water surface level. The study showed that the water surface level measured in the upstream section of the bridge showed no rise condition especially for wider channel section with the flat slope. However, the water surface level measured at the immediate upstream section of the bridge slightly increased and the increasing pattern of water surface level was only noticeable for smaller channel width (20 ft.), especially for increased flow rate.

Keywords: Pier, HEC-RAS, Hydraulic simulation, Water surface elevation

Introduction

Since bridges are one of the most vital and expensive transportation infrastructures (Laursen, 1984), they incur the significant amount of budget for highway agencies for their maintenance and rehabilitation (Purvis, Ronald L et al., 1994). Piers are an important substructure of the bridges and typically restored and reused through the pier encasement in order to extend its useable service life. However, pier encasement may increase its diameter resulting into the negative consequences on hydraulic performance. With the increase in pier width due to encasement, the water surface elevation at the bridge vicinity may increase. Consequently, the increase in water surface elevation might create an additional problem of flooding near the bridge sites, which are especially located in high-risk flood zones. Flooding near the bridges are very common and there are several documented studies of bridge flooding in the past (Naudascher and Medlarz, 1983; Malavasi and Guadagnini, 2003; Palermo and Nistor, 2008). For example, 73 bridges were destroyed by flooding in Pennsylvania, Virginia and West Virginia (Richardson et al., 1993) in 1985.

Flooding is one of the most common forms of natural calamity as it not only takes the lives of thousands of people but also destroys millions of dollars' worth properties each year (Basha et al., 2007). Flood accounts for most human lives and property loss (around 90%) (Krimm 1996) in the United States compared to all other natural calamities. As a result, the National Flood Insurance Program (NFIP) was established in 1968, especially after the promulgation of the National Flood Insurance Act in order to address the recurring flood damage in these flood prone areas (Gary et al., 2003). The NFIP Zone AE is the high-risk flood plain, which can be inundated by a 1% annual chance of flooding (100-year storm) and whose base flood elevations have been determined. If a bridge and its piers are located within the defined floodway boundaries of a Federal Emergency Management Administration (FEMA) NFIP Zone AE, certain restrictions apply. That is, bridge piers in Zone AE must maintain a no-rise condition in terms of water surface elevations because of repair or replacement work such as pier encasement.

The water surface elevation difference between the floodway elevation and the 100-year base flood elevation at any cross section is termed as flood surcharge (Gary et al., 2003). It usually varies from cross section to cross section. The floodway surcharge limit set by FEMA standard is not to exceed 1.0 ft (0.3 m) at any cross section. In general, smaller the allowable rise, the portion of floodplain labeled, as the floodway would be large.

For analyzing such flood and identifying the flood inundation zone, typically the hydraulic modeling is conducted using the Hydrologic Engineering Center's River Analysis System (HEC-RAS) software (Pappenberger et al., 2005; Di Baldassarre et al., 2009a). The suitability and reliability of HEC-RAS in simulating floods in natural streams and rivers is well documented (Horritt and Bates, 2002; Anderson et al., 2002). It also serves as an excellent tool for hydraulic modeling near the bridge sites (Dyhouse et al., 2003; Seckin et al., 1998; Hunt et al., 1999)

While several studies in the past have been conducted using HEC-RAS for flood analysis, the pier encasement effect and its effect on additional flooding have not been explored yet. The pier encasement may affect the flow in two ways: i) due to the obstruction of flow; ii) due to the change in the shape of the encasement. The Drag Coefficient (C_D) and the Yarnell Coefficient (K) typically used in calculations during the hydraulic analysis may change due to the change in pier shape. For example, Suribabu et al. (2011) reported that the flow, width including the shape of the pier and its position in the river might have a significant role in drag characteristics. El-Alfy (2009) also reported that the discharge value, type of flow, pier shape coefficient and the geometrical boundaries of the cross-section at the bridge site could be the main reasons for backwater rise on the bridge upstream. While it has been clear to the scientists for several years that the channel obstruction causes backwater effect, the backwater effect caused by the pier encasement and its additional effect on flooding is still unknown (Charbeneau and Holley 2001). Therefore, the quantification of pier encasement effect on headwater elevation is essential for different channel configurations. In this context, the objective of this study was to quantify the effect of bridge pier encasement on water surface level near the bridge vicinity, which could be helpful to detect any additional rise of water surface level near the flood plain, especially during a flooding period. For this, the hydraulic simulations were conducted for various channel configurations and pier sizes using HEC-RAS.

Theoretical Description

HEC-RAS was developed by the United States Army Corps of Engineers-Hydrologic Engineering Center (USACE-HEC), which has been widely used to examine the impact of various river structures such as bridges, culverts, dams, and weirs on water surface profiles. It is a modern advanced computer program designed to handle a number of hydraulic computation in a single run in a Graphical User Interface (Brunner, 2010). Currently, the tool is extended to water quality analysis besides its application to the unsteady flow simulation, sediment transport models, ice hydraulics, multiple bridge and culvert opening analysis.

HEC-RAS solves standard step method to calculate water surface profile, which is an iterative process of computing water surface elevation by balancing the energy equation at each cross section. In its simplest form, the energy equation is defined as the sum of the pressure, elevation and the velocity head for any cross section. This equation was developed originally for flow under pressure and emerged as energy equation for pressure conduits.

$$Z_2 + \frac{P_2}{\gamma} + \frac{V_2^2}{2g} = Z_1 + \frac{P_1}{\gamma} + \frac{V_1^2}{2g} + h_e \qquad (2.1)$$

Where Z_1 and Z_2 are elevations of the conduit centerline (ft), P_1 and P_2 are the pressure of the fluids; V_1 and V_2 are mean velocities in the pipe, γ the specific weight of fluids (lb/ft^3). Similarly, g is acceleration due to gravity, and h_e is energy head loss between downstream and upstream point.

HEC-RAS also solves momentum balance method to calculate water surface profile, where momentum balances are computed in bridge opening between the four cross sections such as bridge upstream, bridge downstream, and immediate bridge upstream and downstream, respectively. The momentum balance method takes place in three steps: i) first from bridge immediate downstream cross section to bridge downstream inside the bridge; ii) second, from bridge downstream to bridge upstream inside the bridge; iii) and finally from bridge upstream to the immediate upstream cross-section. In a momentum balance method, the force of water moving around the piers is estimated by drag coefficient. Lindsey (1938) through experimental data provided drag coefficients for the different pier shapes. The Table 2-1 below shows few characteristic drag coefficient values that are usually adopted for piers.

In HEC-RAS, standard step method is most often used for the computation of water surface profiles at any river section. The Standard step method encompasses energy, continuity, and Manning's equation to find out the depth and water headwater elevation at various locations along the stream. The equation assumes that the flow is steady, gradually varying, one-dimensional, on a small slope (less than 10%) and under hydrostatic pressure. Moreover, the geometry, roughness value, discharge, coefficients of expansion and contraction and boundary conditions (starting water surface elevation and flow regime) must be specified in order to run the program using standard step method. The process of computation is iterative, especially due to the non-linearity of the equations, which require trial and error solution at every cross section.

Materials and Methodology

Bridge Pier Encasement

The types of piers used for waterway bridges include capped pile type piers, cap-and-column type piers, and solid wall or T-type piers (ODOT Bridge design manual, 2007). The ease of removal of debris at the pier face is a determining factor while choosing the type of pier to be used. Therefore, T-type piers are not typically recommended as it is very difficult to remove debris from them (ODOT Bridge design manual, 2007). Rather, H-pile and concrete pile piers will be an appropriate choice in such conditions. The Figure 2-1 a) shows the typical H-piles used in Ohio state bridges. Pier encasement is one of the rehabilitation methods often used to allow the reuse of existing pile piers during the repair, where an existing pile pier is enclosed with a polyethylene or PVC pipe large enough to provide at least three inches of concrete cover over the existing pier when filled. One-inch wide stainless steel bands are also wrapped around the pipe at one-foot spacing and are tightened enough to prevent any elongation during placing of concrete into the pipe. Figure 2-1 b) shows the typical H-piles after encasement.

Overall Modeling Approach

HEC-RAS is one of the most popularly used tools for hydraulic simulation near bridge site to evaluate the backwater effects mainly due to its accuracy in modeling natural streams with negligible cost (Castellarin et al., 2009). It uses two cross sections upstream and two cross sections downstream of the pier, from the centerline of the channel for hydraulic analysis near the bridge site (Brunner, 2010). Figure 2-2 shows the typical channel profile and cross section locations. Cross-Section 1 is positioned adequately downstream from the structure, whereas Cross-Section 2 is located slightly downstream of the bridge (downstream toe of the embankment). Cross-Section 3 is placed marginally upstream of the bridge (upstream toe of the embankment). However, Cross Section 4 is the farthest upstream cross section. The contraction length (Lc) is referred to the distance between Cross-Section 3 and Cross-Section 4, and the expansion length (Le) is referred to the distance between Cross-Section 1 and Cross-Section 2. Typically, the contraction length (Lc) is less than expansion length (Le) and depending upon the high flows investigation expansion length is determined. Generally, Lc is adopted as the average obstruction length, and Le is typically determined after field investigation, which depends on the degree of constriction, slopes, and roughness of overbank/channel. Once an expansion ratio is selected, it will be multiplied by Lc to determine Le.

HEC-RAS offers few options for water surface profile computations. One of the methods generally used for water surface profile computation is an equation suggested by Yarnell (Yarnell, 1934). Yarnell developed an empirical equation based on 2600 experiments, which were conducted on large channels. Yarnell did not include all possible pier shapes in his experiment; rather his experiments were mostly relying on rectangular and trapezoidal piers. Since his equation was developed mainly for specific conditions, this method may not be applicable unless the case study falls within the data range of his experiment. Moreover, the equation is used if the energy loss is particularly due to piers since it is sensitive to the shape of the pier, and water flow velocity (Brunner, 1995).

The energy and momentum methods are suitable for various flow conditions. However, both methods have some limitations. For example, energy method takes into account the loss through the contraction and expansion but does not take into account the losses due to the shape of the pier. The momentum method considers the losses due to drag forces in the pier but this method calculates the weight force using an average bed slope, which is practically not possible to compute for natural cross-sections.

Since the goal of this research was to investigate the effect of pier encasement on the rise in headwater elevations, high flow computations in HEC-RAS were implemented either using the energy equation method or by using pressure and weir flow methods. In the pressure and weir flow methods, HEC-RAS automatically uses the suitable type of equations based on the flow situation. For example, HEC-RAS uses two types of orifice flow depending upon the flow condition: i) when the water touches only the upstream side of the bridge section; ii) when the bridge constriction is flowing completely full (HEC-RAS 2010). In summary, the following methods should be used for high flow methods.

- The energy method should be used if a bridge deck creates little or no obstruction for the passage of water and bridge opening is not behaving as if it is a pressurized orifice.

- The pressure and weir method could be an appropriate choice when the bridge deck creates a significant obstruction to the flow.

The energy-based method is selected if the bridge is significantly immersed and flow is not behaving like weir flow. Whereas, momentum method is selected if significant drag losses are expected near the pier.

HEC-RAS Model Inputs

All channel and pier configurations were run in non-encased and encased conditions for comparison assuming the flow was contained within the channel geometry. The study was conducted using typical trapezoidal cross sections of the rivers. The study was limited to only two kinds of piers; H-piles and round concrete pile piers. Moreover, the shape of pier encasement to be provided was round. The pier encasement data to be incorporated into the HEC-RAS analysis were adopted using ODOT document, which is attached in Table 2-2. The multiple numbers of piers with varying shape (circle and square) experimented in HEC-RAS, and the parametric study was performed by analyzing pre- and post-encasement water surface elevations under varying channel conditions. The generic flat bottom channel section with 2:1 side slopes and the manning's roughness coefficient (n) of 0.035 was considered for all the channel configurations. The drag coefficient constant for circular and square pier was taken as 1.2 and 2, respectively. In addition, the model was developed for nine different bottom widths varying from 20 ft to 180 ft at 20 ft. interval for the various river slope conditions such as 0.3%, 0.5%, 0.7% and 1.0%. For the same geometric configuration, the study was conducted using two and three number of pier rows by maintaining the minimum span of 18 ft and a maximum span of 58 ft between two piers. This limited the use of pier numbers depending upon the size of channel width in consideration. For example, for the smaller channel bottom width such as 20 ft, two piers were sufficient. However, the bigger bottom channel width such as 140 ft, 160 ft, and 180 ft could accommodate three numbers of piers. The flow discharge was chosen according to the channel carrying capacity and it ranged from 200 cfs to 20,000 cfs.

Model Establishment

A flat bottom generic channel section of side slope 2:1 with varying widths and number of piers (two and three) was developed in HEC-RAS in order to see the effect of bridge pier encasement on water surface level. The Manning's roughness coefficient of 0.035 was taken for the channel section. Since HEC-RAS requires a minimum of four cross-sections for the simulation of water surface level near the bridge, numerous cross-sections were developed by creating two cross-sections at first and then interpolating them equally into certain numbers depending upon the reach length. The suitable reach length was adopted based on the width of the channel bottom in consideration. For example, reach length of 500 ft was considered for channel bottom width of 180 ft and decreased subsequently as the channel width was decreased. The typical channel cross-section in HEC-RAS with 180 ft bottom width is shown in Figure 2-3. Similarly, the location of immediate upstream and most upstream site of the bridge for various reach length under consideration is shown in Table 2-3.

Water surface elevations were computed using energy equation (standard step method) available in HEC-RAS model. Two piers were used for the channel of 20 ft bottom width, whereas analysis was accomplished using both two and three piers separately for the channel bottom widths of 40 ft to 120 ft. Similarly, three piers were used from 140 ft to 180 ft channel bottom width in order to maintain the ODOT's typical recommended distance between two piers (minimum 18 ft and maximum 58 ft span). Initial flow was provided for producing a depth of minimum 3 ft and maximum 10 ft depth for the specific channel geometry of 2-pier row and 3-pier row configurations. We increased the flow volume at 200 cfs increments up to the maximum possible flow that could be practically accommodated by the given channel size. This resulted in 224 various models including both encased and non-encased pier conditions. Figure 2-3 shows one such example of a model of bottom width 180 ft with several channel cross sections. Similarly, Figure 2-4 shows the bridge cross-section with pier location in the channel of 180 ft bottom width.

Results

The difference in water surface elevation for existing and proposed pier encasement for various channel widths and slopes were calculated exclusively by standard step method in HEC-RAS using a mixed flow regime even though the experiment was conducted with momentum and Yarnell method. The data were documented for both no-rise and rise condition. Different States in the US have defined the range of no-rise and rise condition depending upon the allowable surcharge limit of the flood. Table 2-4 shows that the allowable state surcharge limits of 0.5 ft as the no-rise condition for Ohio. Therefore, this threshold of 0.5 ft was used for each channel configurations to identify the no-rise and rise condition.

Table 2-5 shows no-rise condition for the circular pier using two and three piers for all channel configurations for the ranges of flow that each channel could accommodate. For example, a 20 ft. channel bottom width with a slope of 0.3% and two piers showed no-rise condition for flow range up to 5600 cfs at the immediate upstream cross-section of the bridge. Similar conditions (no rise condition) were observed in most upstream cross-section for the flow range up to 5600 cfs. The flow was limited to 5600 cfs as it was the maximum discharge that the channel could accommodate. We conducted the analysis for another channel slope including 0.5%, 0.7%, and 1%. Our analysis indicated that the rise condition would be realized for higher slope even if the smaller flows are considered. For example, rise condition would be experienced after 2400 cfs and 1400 cfs, for the channel of 0.5% and 0.7% slope, respectively (Table 2-5).

For a channel of 40 ft bottom width with the slope of 0.3%, no rise condition was detected up to the flow range of 8400 cfs. This was true regardless the number of piers (two and three) that had been chosen. Similarly, for a channel of bottom width 40 ft and the longitudinal slope of 0.5% (two piers), the no-rise condition was experienced for the flow up to 8400 cfs at the most upstream cross-section and for the flow up to 6800 cfs at immediate bridge upstream. The flow was limited to 8400 cfs as it was the maximum discharge that could be occupied by the channel of 40 ft bottom width. As the slope was increased, the rise condition was realized even for the relatively lesser flows. For example, for 0.7% and 1% channel slope with two piers bridge system, the rise condition was experienced for flows greater than 7600 cfs and 3800 cfs, respectively. The detail ranges of the flows for a no-rise condition for various channel configurations has been reported in Table 2-5. Any values exceeding the flow ranges that has been reported in Table 2-5 for the respective channel configurations would produce the rise condition.

Similarly, Table 2-6 depicted a no- rise in water surface elevation for square piers for two and three piers case for all channel configurations. The rise in headwater elevation was significantly affected by the pier width as the rise in water surface elevation was clearly noticeable with the increase in pier width. Since the increased pier width further creates the obstruction for the flow, it is not surprising to see such increase in the water surface elevation. Moreover, the effect was significant for smaller channel width and greater slope relative to bigger channel width and lesser slope.

The rise in water surface elevation also was greatly affected by the flow volume in the river cross-section. For example, the difference in water surface elevation for existing (before encasement) and proposed pier (after encasement) for the channel section of 20 ft and 1.0% slope was much lesser for 200 cfs (0.02 ft) when compared to flow volume 5000 cfs (0.98ft) (not shown in the figure). This was mainly because the higher flow volume occupied more channel area; therefore, even a small obstruction to its flow made a significant change. In general, the water surface elevations after the encasement were found to be slightly increased depending upon the flow volume under consideration. This modest increase in water surface elevation was noticeable for higher flow volume compared to lower flow volume.

The slope of channel section also greatly influenced the headwater elevation. For example, the difference in water surface elevation for existing and proposed pier encasement for the channel section of 20 ft channel section was greatly affected by slope even for the same discharge. For example, a 0.3% channel slope with the discharge of 5000 cfs showed a lesser rise in water surface elevation (0.23 ft) when compared to the slope of 0.7% and 1.0% slope (0.88 ft and 0.98 ft, respectively). Typically, the differences in water surface elevation were higher for 0.7% and 1.0% slope when compared to 0.3% channel slope indicating that the steeper channel could produce higher water surface elevation compared to flatter slopes.

Channel bottom width was another channel property, which affected the water surface elevation. For example, the difference in water surface elevation for existing and proposed pier for the channel section of 20 ft bottom width with 1.0% channel slope and 5000 cfs flow showed a greater rise in water surface elevation (0.98 ft). However, for a channel of 180 ft bottom width with the same channel section properties and flow (5000 cfs), the rise in water surface elevation was significantly less (0.01 ft).

HEC-RAS also generates profile plots displaying the water surface elevation, energy grade line, critical depth, bank stations etc. The profile plot for the existing and proposed pier of 20 ft. channel bottom width with 1% channel slope is shown in Figure 2-5 and Figure 2-6, respectively. The Figure 2-7 shows the difference in water surface elevation at most bridge upstream for all the flows (200 cfs-5600 cfs) for 20 ft bottom width with two circular piers for the entire four channel slopes. The channel section with 0.3% slope showed no rise for all the possible flow ranges. Then as the slope was increased, rise condition started to appear. For example, the rise condition was detected after 2400 cfs for 0.5% slope, whereas the rise condition was observed shortly after 1400 cfs for both 0.7% and 1% slope. The Figure 2-8 shows the difference in water surface elevation at immediate bridge upstream for the 20 ft channel section for all the flows. A similar trend was detected with 0.3% channel slope indicating no rise conditions for all the flows. However, it started gradually increasing as the slope was progressively increased. For example, the rise condition appeared for 0.5% slope at flows greater than 1800 cfs, whereas the rise condition appeared for 0.7% and 1.0% slope at flows greater than 800 cfs.

Figure 2-9 shows the difference in water surface elevation at most bridge upstream for all the flows (200 cfs-15000 cfs) for 100 ft bottom width with 2 circular piers. It covers the entire four channel slopes considered for the analysis. Channel section with 0.3%, 0.5% and 0.7% slope showed no rise for all the possible flow ranges. However, as the slope was increased to 1.0%, rise condition started to appear. When flow was increased from 11400 cfs to 11600 cfs, there was an abrupt rise from 0.32 ft to 0.72 ft and later the same gradual increasing trend was continued. The Figure 2-10 shows the difference in water surface elevation at immediate bridge upstream for the same channel section for all the flows. The trend remained similar with 0.3% and 0.5% slope showing no rise for all the flow ranges. However, as the slope was increased, the rise condition appeared for 0.7% and 1.0% slopes for higher flows after 14000 cfs and 10600 cfs, respectively.

Figure 2-11 and Figure 2-12 show the difference in water surface elevation at most bridge upstream and immediate bridge upstream respectively for all the flows (200 cfs-20000 cfs), for channel section of 180 ft bottom width comprising three circular piers. It showed a no rise condition in both the cross section for all the flow ranges regardless of the channel slopes. For the conciseness of the manuscript, we have not reported the graphical plot of water surface elevation vs. flows for all channel width. However, the rise condition and no-rise condition for each channel configurations have been tabulated. Nevertheless, the change in water surface elevation obtained at various channel bottom width due to loss in area after encasement has been plotted in figure 2-13. The Table 2-5 shows the no-rise condition for the circular pier, whereas the Table 2-6 shows the no-rise condition for the square pier. The rise condition will be experienced for all flows exceeding the flow limits specified in Table 2-5 and Table 2-6. In table, The fourth column shows the flow range used for analysis for particular bottom channel width. The fifth and sixth column indicate the flow range for which the no-rise condition was detected at most upstream and immediate bridge upstream respectively.

The analysis indicated that there was an increase in water surface elevation after encasement due to the increase in discharge. In addition, increased slope also produced a greater rise in water surface elevation after the encasement. The study suggested that the channel of 180 ft bottom width did not show any rise in water surface elevation even with the maximum discharge. Moreover, even the higher slope did not have any substantial effect on water surface elevation in a wider channel. In general, the wider channel provided bigger volume for the water to flow; therefore, the obstruction in such channel showed relatively lesser water surface elevation. Typically, the no-rise conditions were prevalent in wider bottom channel width, whereas the rise conditions were observed in the channel of narrow bottom width. In addition, higher slope and greater discharge enhanced the water surface elevation after the encasement. Apart from Standard Step method, other computational methods like Momentum and Yarnell method were also used to see the effect of pier case encasement in water surface elevation (not shown). However, we did not find much difference in the result no matter what the method was adopted. In fact, the pattern of rise and no-rise condition obtained using standard step method was comparable with other methods such as Momentum and Yarnell method.

Conclusions

The rise in water surface elevation may create a problem in bridge piers located at high-risk flood zone during pier encasement. In this study, the user-friendly HEC-RAS software was utilized to test and implement the different encasement scenario. For every channel, four models were constructed using four different slopes (0.3%, 0.5%, 0.7% and

1.0%). Each channel configuration was modeled twice: one without pier encasement (existing); and other with pier encasement (proposed). Therefore, more than 220 models with different channel configurations and piers were modeled and water surface elevation was simulated. Finally, we found out that, the increase in water surface elevation after pier encasement was a function of the width of the pier, flow volume, channel slope, and channel bottom width. The sections with small width, high slope and high flow are at highest risk.

With encasement, the pier width increased resulting in the further constriction of the channel and increased water surface elevation. The effect was significant for smaller bottom width and steeper channel slopes. With the increase in the channel slope, there was a rise in the water surface elevation regardless of the channel width. For example, the steeper channel slopes such as 0.7% and 1.0% showed the maximum rise in water surface elevation after the pier encasement even for smaller flow rate. Whereas the flatter channel slope like 0.3% and 0.5% showed a comparatively lesser rise in water surface elevation after pier encasement. Moreover, the bottom width of the channel had a vital effect on water surface elevation. For wider bottom width, the rise in water surface elevation after the pier encasement was nominal. For example, the channel bottom of 180 ft showed a negligible rise in water surface elevation after the pier encasement. This was true even for steeper slopes (0.7% and 1.0%). Whereas for smaller bottom width, the rise in water surface elevation after the pier encasement was significant. For example, the channel bottom of 20 ft relatively showed a tremendous rise of water surface elevation than 180 ft after the pier encasement. In addition, flow also had a substantial effect on increased water surface elevation, which was clearly noticeable after the pier encasement.

Furthermore, the difference of water surface elevation for existing and proposed pier configuration was computed for all the channel sections. The computed difference was broadly categorized into the rise and no-rise conditions depending upon the simulated water surface level in the upstream section of the bridge. The rise and no-rise condition were declared as per Ohio standards, which considers the no-rise condition if the increased water surface elevation was limited to 0.5 ft.

Finally, this study may be beneficial and serve as a guideline for rehabilitation practices like bridge pier encasement in flood prone areas. The study also shows the effect of slopes, flow and channel bottom width on water surface elevation after the pier encasement, which might be very helpful for concerned state and federal agencies to take necessary protection measures in the highly flood-prone zones.

References:

Anderson, M. L., et al. "Coupling HEC-HMS with Atmospheric Models for the Prediction of Watershed Runoff." Building Partnerships. 2000. 1-10.

Basha, Elizabeth, and Daniela Rus. "Design of early warning flood detection systems for developing countries." Information and Communication Technologies and Development, 2007. ICTD 2007. International Conference on. IEEE, 2007.

Brunner, Gary W. "HEC-RAS (River Analysis System)." North American Water and Environment Congress & Destructive Water: ASCE, 2010.

Brunner, Gary W. HEC-RAS River Analysis System. Hydraulic Reference Manual. Version 1.0. Hydrologic Engineering Center Davis CA, 1995.

Charbeneau, Randall J., and Edward Raymond Holley. Backwater effects of bridge piers in the subcritical flow. Center for Transportation Research, Bureau of Engineering Research, the University of Texas at Austin, 2001.

Di Baldassarre, Giuliano, et al. "Probability-weighted hazard maps for comparing different flood risk management strategies: a case study." Natural Hazards 50.3 (2009): 479-496.

Dyhouse, Gary, et al. "Floodplain modeling using HEC-RAS." (2003).

El-Alfy, K. "Backwater rise due to flow constriction by bridge piers." Thirteenth International Water Technology Conference (2009): 1295-1313.

HEC-RAS 4.10 User’s Manual. Hydrologic Engineering Center, US Army Corps of Engineers (2010).

Hicks, F. E., and T. Peacock. "Suitability of HEC-RAS for flood forecasting." Canadian Water Resources Journal 30.2 (2005): 159-174.

Horritt, M. S., and P. D. Bates. "Evaluation of 1D and 2D numerical models for predicting river flood inundation." Journal of hydrology 268.1 (2002): 87-99.

Hunt, John, Gary W. Brunner, and Bruce E. Larock. "Flow transitions in bridge backwater analysis." Journal of Hydraulic Engineering 125.9 (1999): 981-983.

Krimm, Richard W. "Reducing flood losses in the United States." International Workshop on Floodplain Risk Management. < The> Committee of International Workshop on Floodplain Risk Management, 1996.

Laursen, Emmett M. "Assessing vulnerability of bridges to floods." Transportation Research Record 950.2 (1984).

Lindsey, Walter Frank. "Drag of cylinders of simple shapes." (1938).

Malavasi, Stefano, and Alberto Guadagnini. "Hydrodynamic loading on river bridges." Journal of Hydraulic Engineering 129.11 (2003): 854-861.

Naudascher, E., and H-J. Medlarz. "Hydrodynamic loading and backwater effect of partially submerged bridges." Journal of Hydraulic Research 21.3 (1983): 213-232.

Oegema, B. W., and E. A. McBean. "Uncertainties in flood plain mapping."Application of Frequency and Risk in Water Resources. Springer Netherlands, 1987. 293-303.

Pappenberger, F., et al. "Uncertainty in the calibration of effective roughness parameters in HEC-RAS using inundation and downstream level observations." Journal of Hydrology 302.1 (2005): 46-69.

Purvis, Ronald L., et al. "Life-cycle cost analysis for protection and rehabilitation of concrete bridges relative to reinforcement corrosion." Contract100 104 (1994).

Merwade, Venkatesh, et al., "Uncertainty in flood inundation mapping: current issues and future directions." Journal of Hydrologic Engineering 13.7 (2008): 608-620.

Richardson, E. V., et al. Evaluating scour at bridges, 2d ed.: US Department of Transportation, Federal Highway Administration, Hydraulic Engineering Circular 18. Publication FHWA-IP-90-017, 1993.

Sean Meddles. Bridge Design Manual Ohio Department of Transportation, 2007.

Seckin, Galip, Recep Yurtal, and Tefaruk Haktanir. "Contraction and expansion losses through bridge constrictions." Journal of Hydraulic Engineering 124.5 (1998): 546-549.

Suribabu, C. R., et al. "Backwater rise and drag characteristics of bridge piers under sub-critical flow conditions." European Water 36 (2011): 27-35.

Palermo, Dan, and Ioan Nistor. "Tsunami-induced loading on structures." Structure magazine 3 (2008): 10-13.

Yarnell, David Leroy. Bridge piers as channel obstructions. No. 442. US Dept. of Agriculture, 1934.

Source: (ODOT ROC 5)

Figure 2-1: H-Pile- a) pier before encasement and b) pier after encasement

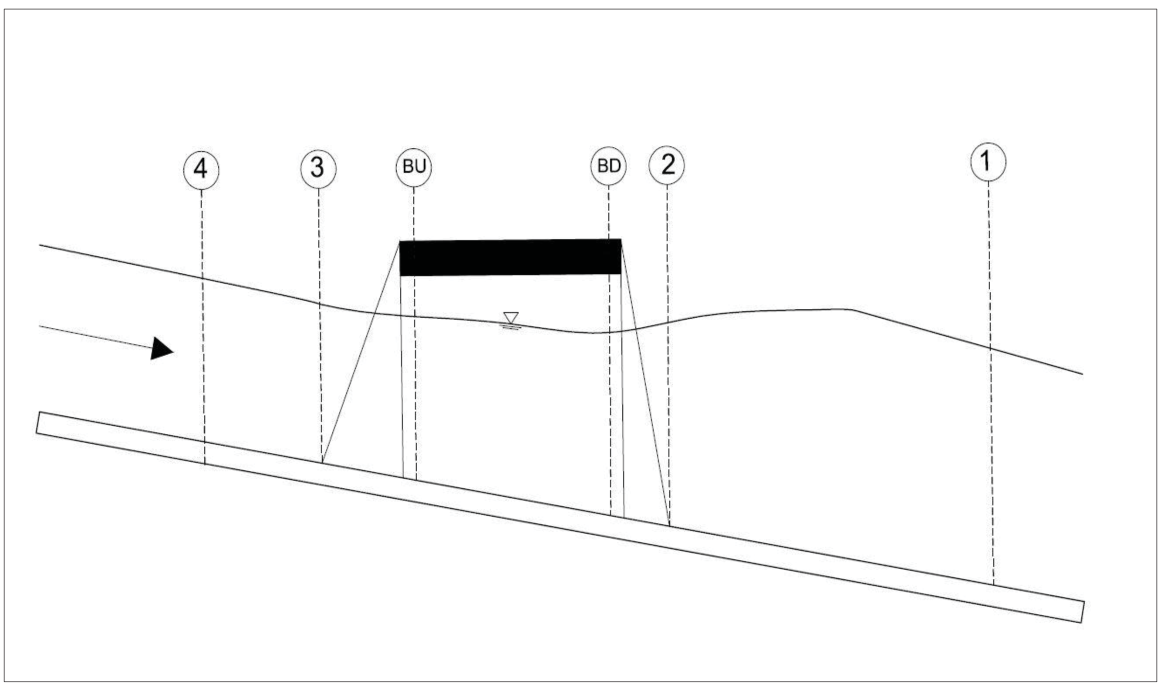

Figure 2-2: Channel profile and cross section locations.

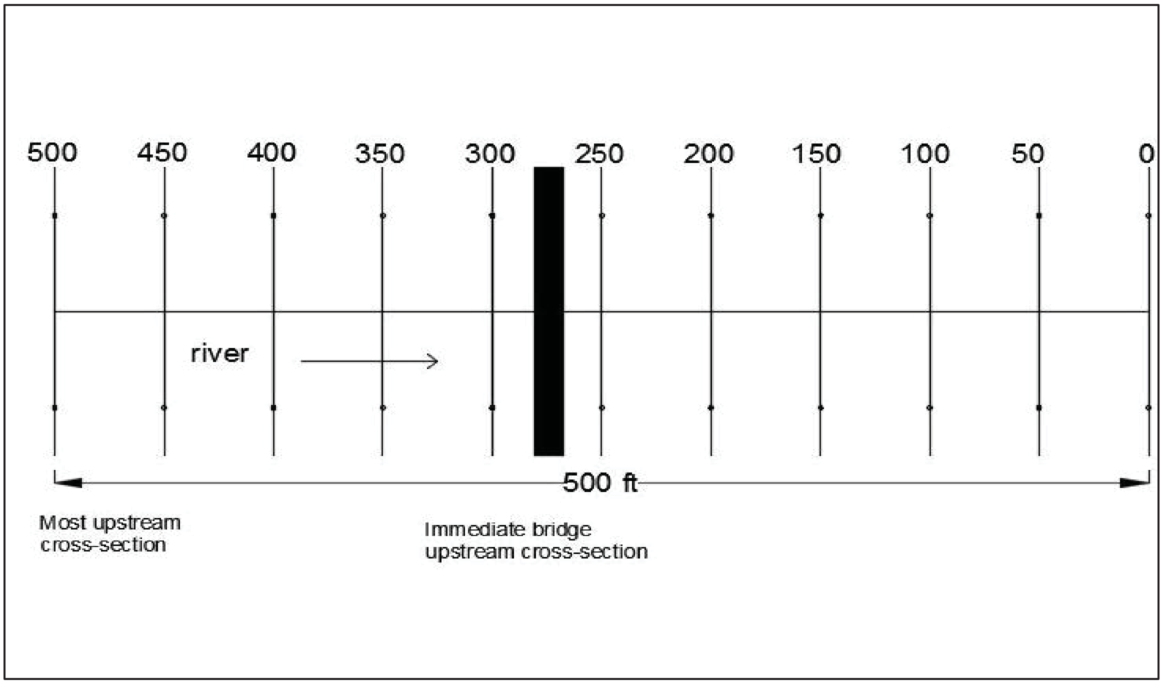

Figure 2-3: Channel cross-section in HEC-RAS with 180 ft bottom width.

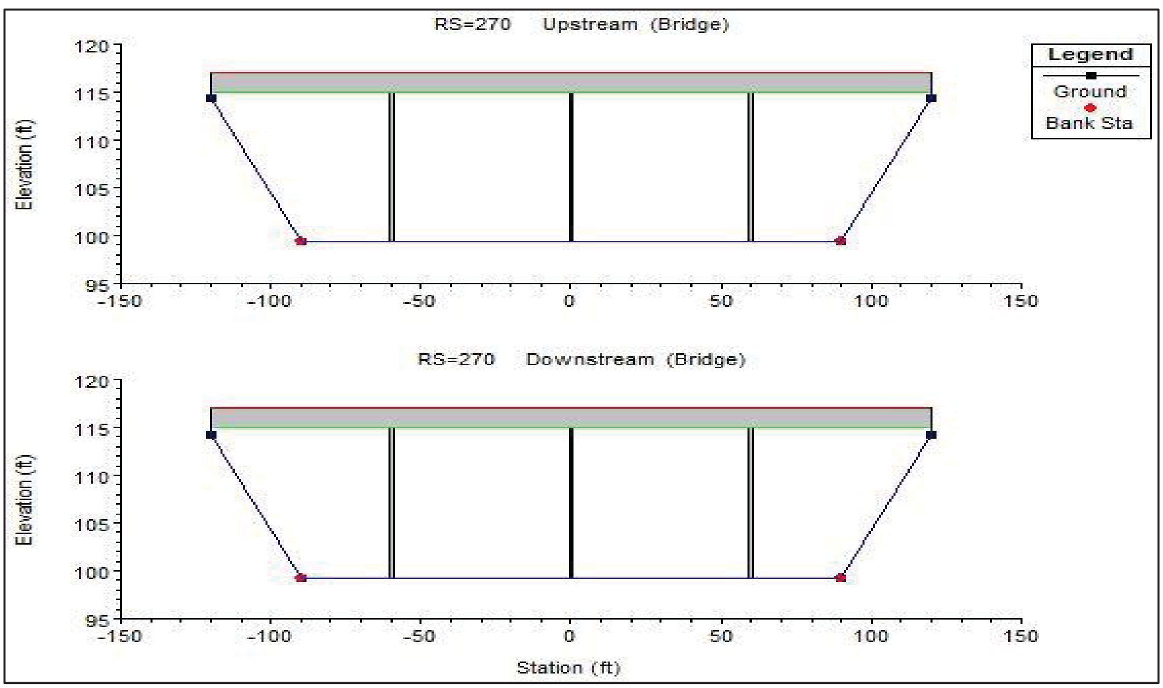

Figure 2-4: Bridge cross-section with pier location in the channel with 180 ft bottom width.

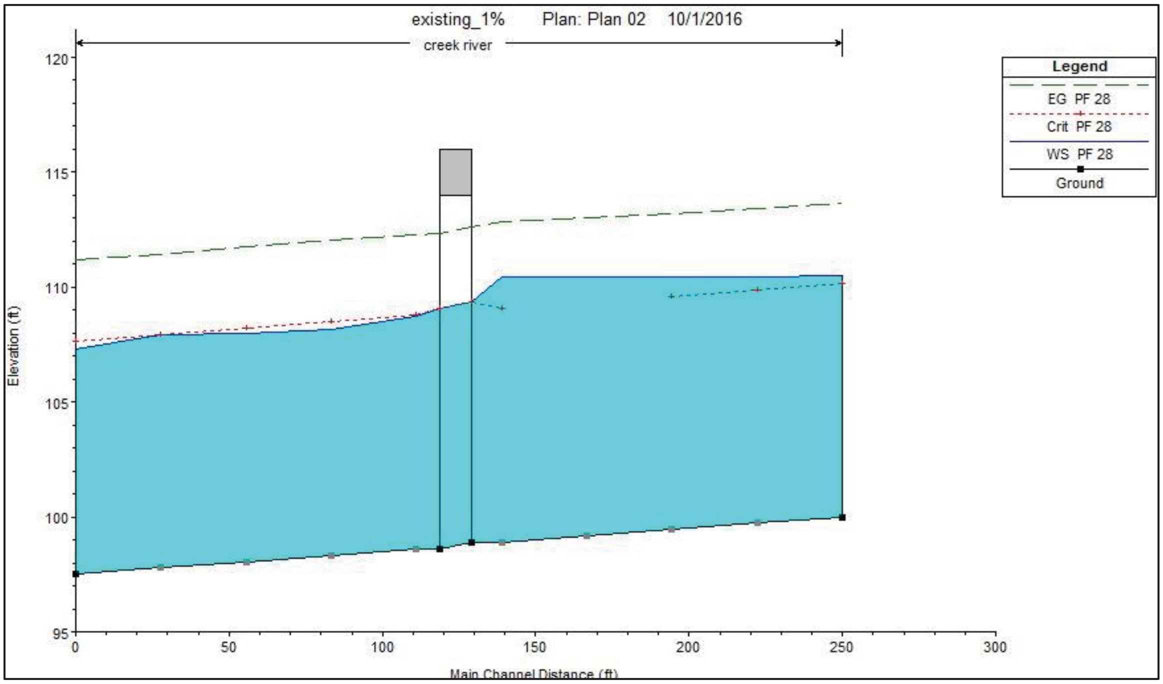

Figure 2-5: Profile plot for 20 ft channel bottom width of 1% channel slope with existing pier.

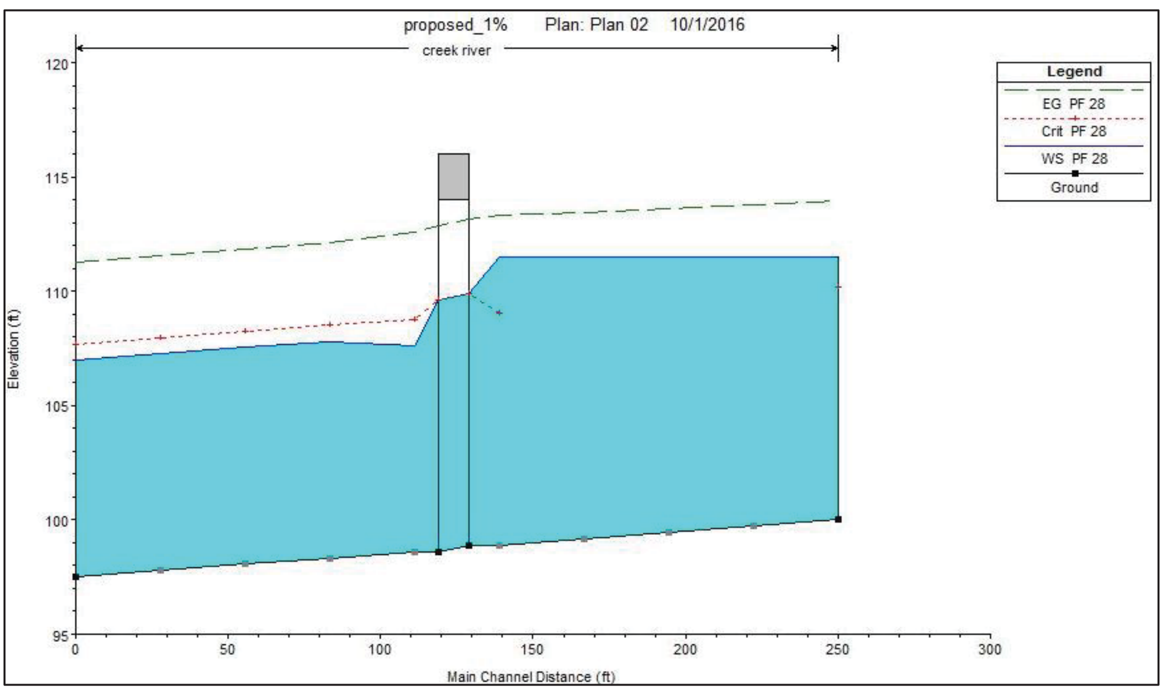

Figure 2-6: Profile plot for 20 ft channel bottom width of 1% channel slope with proposed pier.

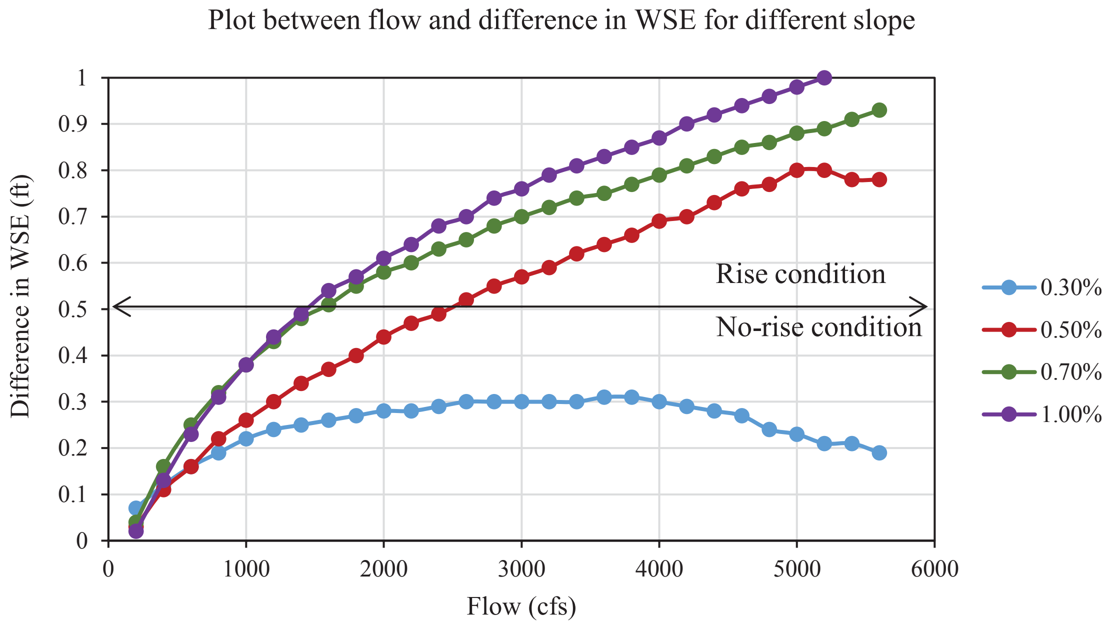

Figure 2-7: The difference in WSE at most upstream for 20 ft channel section.

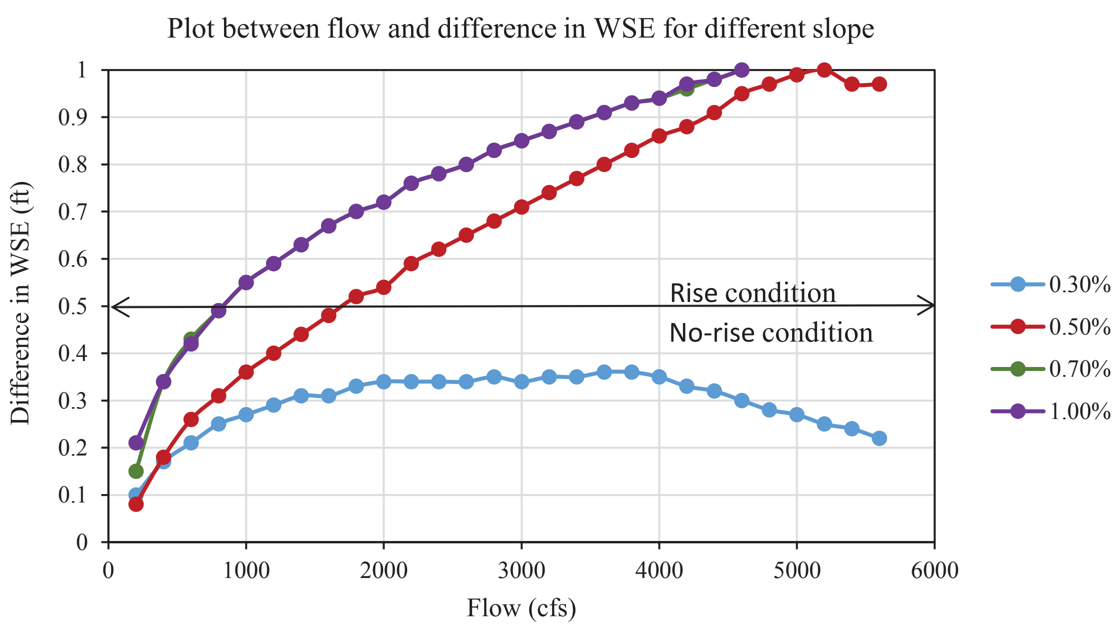

Figure 2-8: The difference in WSE at immediate upstream for 20 ft channel section.

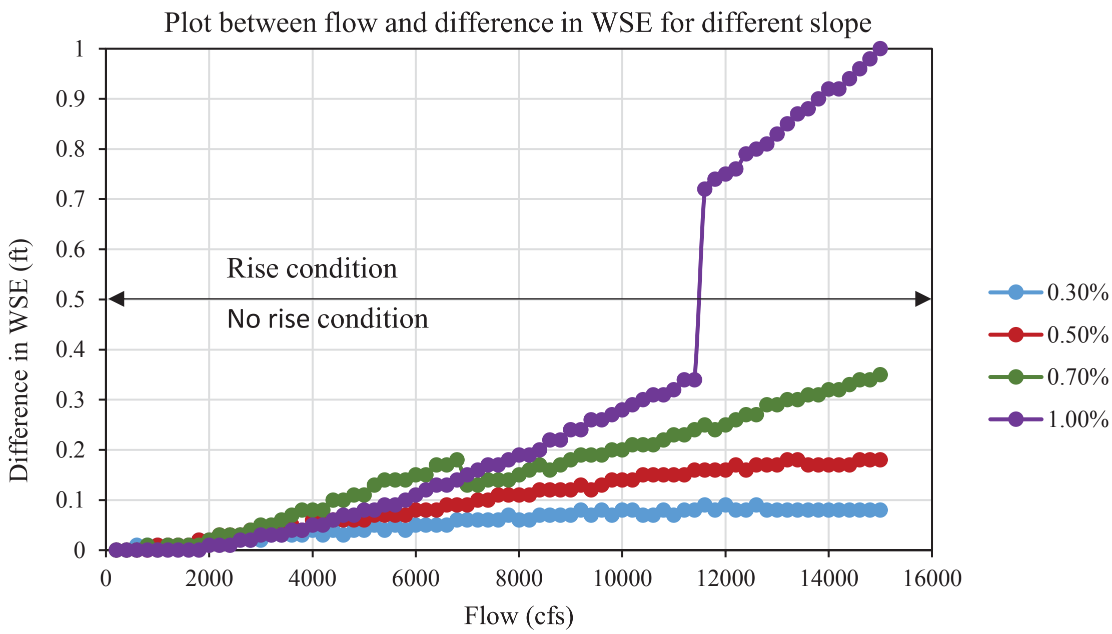

Figure 2-9: The difference in WSE at most upstream for 100 ft channel section.

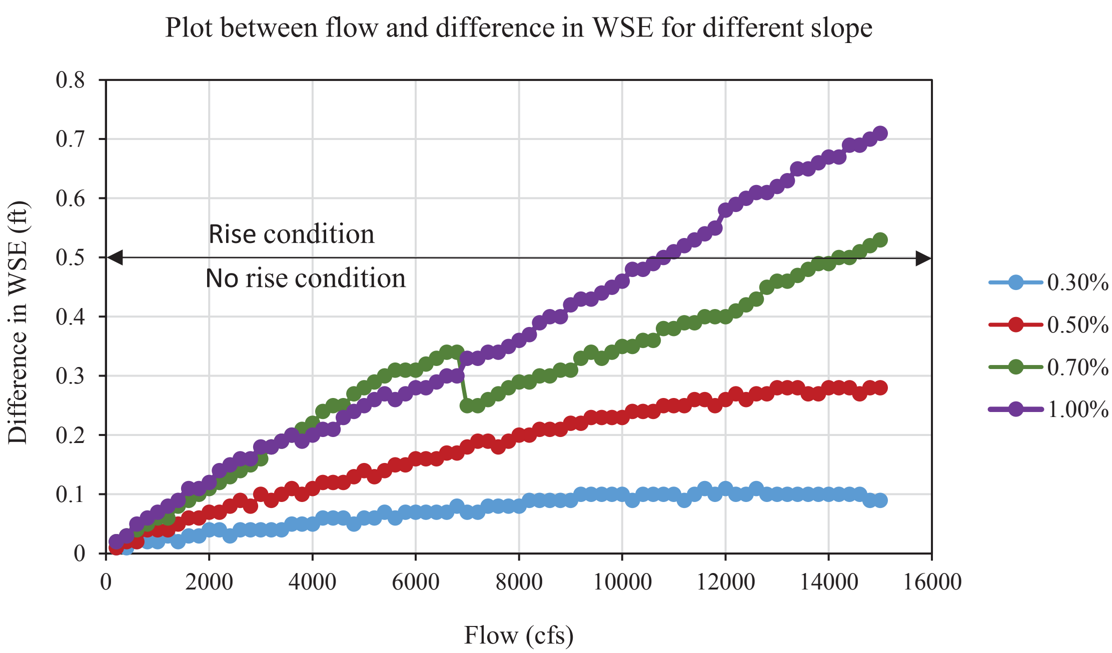

Figure 2-10: The difference in WSE at immediate upstream for 100 ft channel section.

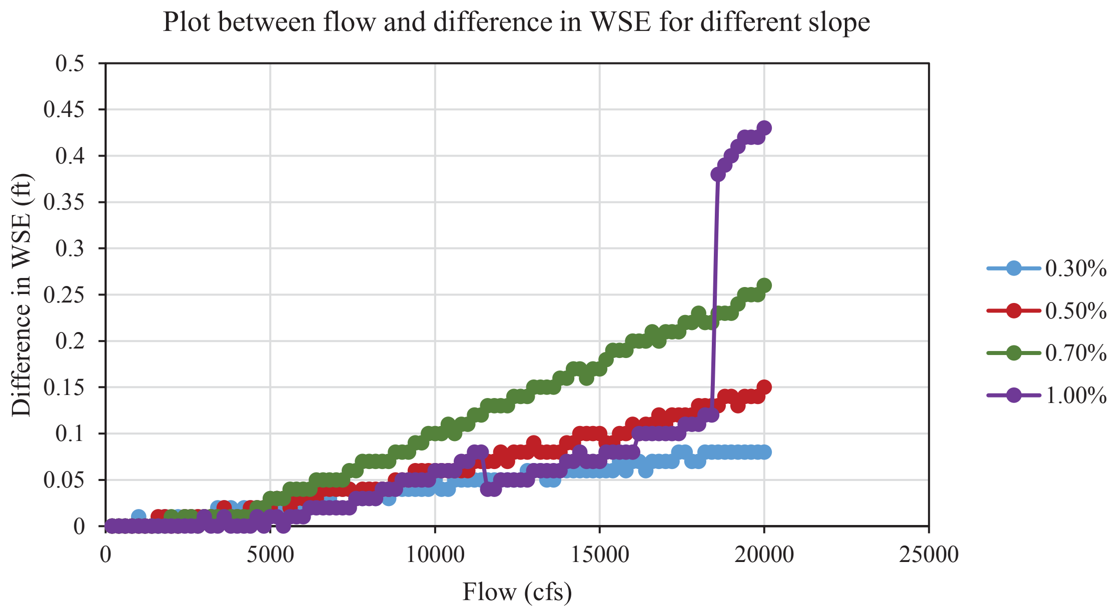

Figure 2-11: The difference in WSE at most upstream for 180 ft channel section.

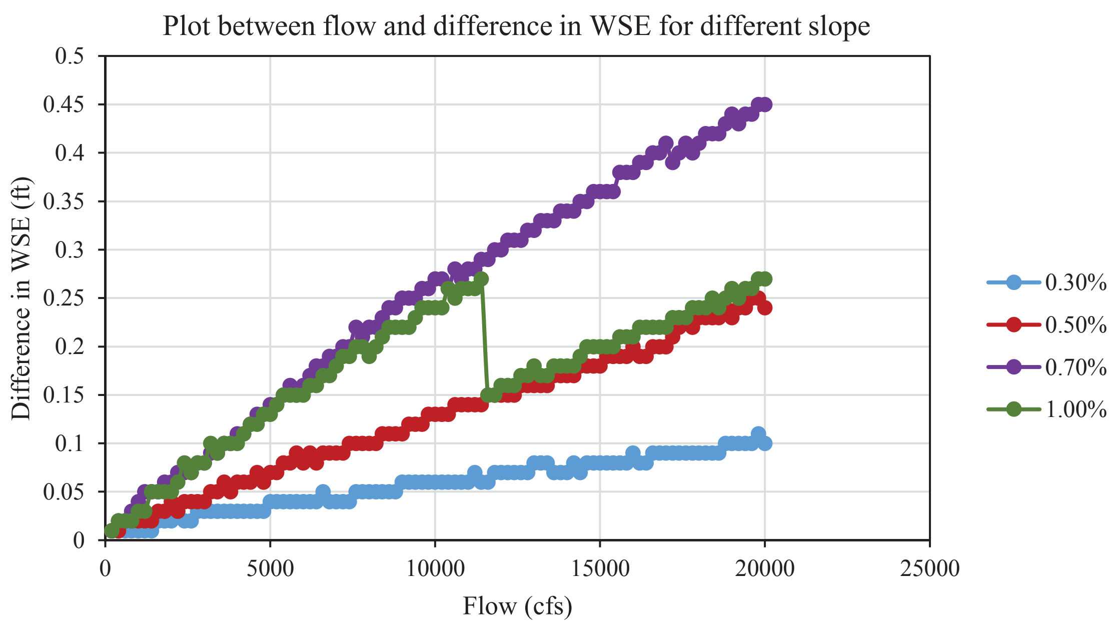

Figure 2-12: The difference in WSE at immediate for 180 ft channel section.

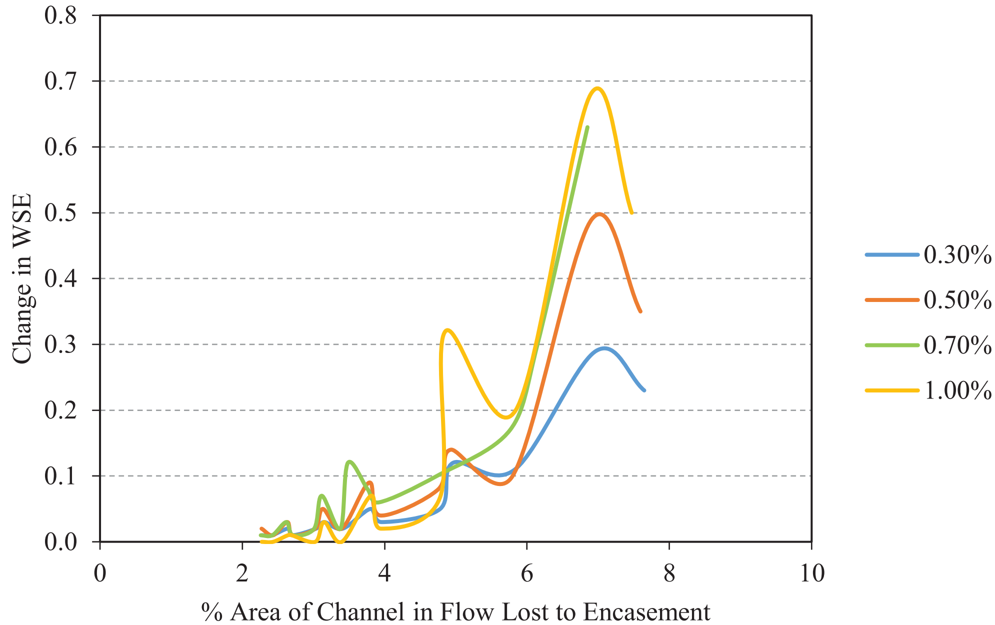

a) For 2400 cfs

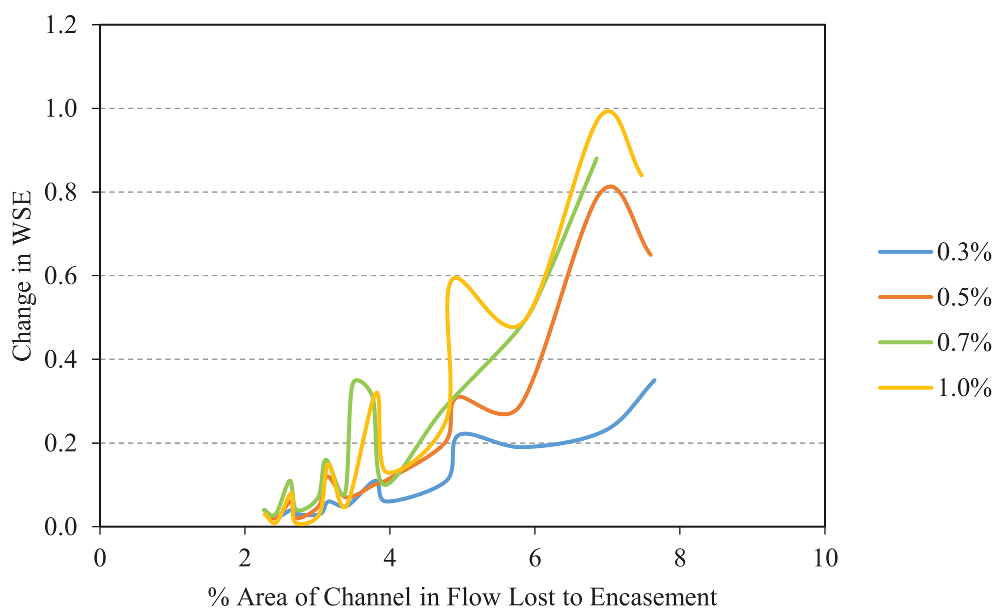

b) For 5000 cfs

Figure 2-13: The difference in WSE with respect to change in area.

Table 2-1: Typical drag coefficients for various pier shapes

Serial No	Pier Shape	Drag Coefficient (CD)
1	Circular pier	1.20
2	Elongated piers with semi-circular ends	1.33
3	Elliptical piers with 2:1 length to width	0.60
4	Square piers	2.00
5	Triangular nose with 30-degree angle	1.00
6	Triangular nose with 120-degree angle	1.72

Table 2-2: Pile pier and encasement data provided by ODOT

Run	Existing size	Shape	Existing type	Encasement	Type	Shape
1	12"	Square	H-Pile	24"ID/28"OD	PE	Round
2	16" OD	Round	Concrete Pile	30"ID/36" OD	PE	Round

Table 2-3: Reach length and location from the centerline of the bridge.

Channel bottom width (ft)	Number of piers	Number of cross-sections	Reach length (ft)	Most upstream from center line of bridge (ft)	Immediate upstream from center line of bridge (ft)
20	2	10	250	125	13.88
40	2,3	10	250	125	13.88
60	2,3	10	300	150	16.66
80	2,3	10	300	150	16.66
100	2,3	11	400	180	30
120	2,3	11	450	205	25
140	3	11	450	205	25
160	3	11	500	225	25
180	3	11	500	225	25

Table 2-4: Allowable state surcharge limits as of 2003 (Gary et al., 2003)

State	**Surcharge (ft)**
Illinois	0.1
Indiana	0.1
Michigan	0.1
Minnesota	0.5
Montana	0.5
New Jersey	0.2
Ohio	0.5 or 1.0*
Wisconsin	0
All other states	1

*Depending on community

Table 2-5: No-rise condition for the circular pier.

Serial No	Bottom channel width (ft)	Flow range (cfs)	Number of piers	Slope (%)	Most upstream cross-section	Immediate bridge upstream cross-section
					Flow (cfs)	Flow (cfs)
1	20	200-5600	2	0.3	Flow ≤ 5600	Flow ≤ 5600
				0.5	Flow ≤ 2400	Flow ≤ 1800
				0.7	Flow ≤ 1400	Flow ≤ 800
				1	Flow ≤ 1400	Flow ≤ 800
2	40	200-8400	2	0.3	Flow ≤ 8400	Flow ≤ 8400
				0.5	Flow ≤ 8400	Flow ≤ 6800
				0.7	Flow ≤ 7600	Flow ≤ 4400
				1	Flow ≤ 3800	Flow ≤ 2600
			3	0.3	Flow ≤ 8400	Flow ≤ 8200
				0.5	Flow ≤ 3600	Flow ≤ 2600
				0.7	Flow ≤ 4000	Flow ≤ 2400
				1	Flow ≤ 2200	Flow ≤ 1400
3	60	200-11400	2	0.3	Flow ≤ 11400	Flow ≤ 11400
				0.5	Flow ≤ 11400	Flow ≤ 11400
				0.7	Flow ≤ 8600	Flow ≤ 5400
				1	Flow ≤ 7800	Flow ≤ 5400
			3	0.3	Flow ≤ 11400	Flow ≤ 11400
				0.5	Flow ≤ 8200	Flow ≤ 6400
				0.7	Flow ≤ 5200	Flow ≤ 3200
				1	Flow ≤ 5000	Flow ≤ 3200
4	80	200-13400	2	0.3	Flow ≤ 13400	Flow ≤ 13400
				0.5	Flow ≤ 13400	Flow ≤ 13400
				0.7	Flow ≤ 12400	Flow ≤ 8200
				1	Flow ≤ 9800	Flow ≤ 8200
			3	0.3	Flow ≤ 13400	Flow ≤ 13400
				0.5	Flow ≤ 13400	Flow ≤ 9800
				0.7	Flow ≤ 8200	Flow ≤ 5400
				1	Flow ≤ 7800	Flow ≤ 5400

Serial No	Bottom channel width (ft)	Flow range (cfs)	Number of piers	Slope (%)	Most upstream cross-section	Immediate bridge upstream cross-section
					Flow (cfs)	Flow (cfs)
5	100	200-15000	2	0.3	Flow ≤ 15000	Flow ≤ 15000
				0.5	Flow ≤ 15000	Flow ≤ 15000
				0.7	Flow ≤ 15000	Flow ≤ 14000
				1	Flow ≤ 11400	Flow ≤ 10600
			3	0.3	Flow ≤ 15000	Flow ≤ 15000
				0.5	Flow ≤ 15000	Flow ≤ 15000
				0.7	Flow ≤ 13800	Flow ≤ 8600
				1	Flow ≤ 9800	Flow ≤ 6000
6	120	200-20000	2	0.3	Flow ≤ 20000	Flow ≤ 20000
				0.5	Flow ≤ 20000	Flow ≤ 20000
				0.7	Flow ≤ 20000	Flow ≤ 20000
				1	Flow ≤ 13200	Flow ≤ 16800
			3	0.3	Flow ≤ 20000	Flow ≤ 20000
				0.5	Flow ≤ 20000	Flow ≤ 20000
				0.7	Flow ≤ 20000	Flow ≤ 20000
				1	Flow ≤ 14200	Flow ≤ 8800
7	140	200-20000	3	0.3	Flow ≤ 20000	Flow ≤ 20000
				0.5	Flow ≤ 20000	Flow ≤ 20000
				0.7	Flow ≤ 20000	Flow ≤ 19000
				1	Flow ≤ 17000	Flow ≤ 15200
8	160	200-20000	3	0.3	Flow ≤ 20000	Flow ≤ 20000
				0.5	Flow ≤ 20000	Flow ≤ 20000
				0.7	Flow ≤ 20000	Flow ≤ 17600
				1	Flow ≤ 18200	Flow ≤ 20000
9	180	200-20000	3	0.3	Flow ≤ 20000	Flow ≤ 20000
				0.5	Flow ≤ 20000	Flow ≤ 20000
				0.7	Flow ≤ 20000	Flow ≤ 20000
				1	Flow ≤ 20000	Flow ≤ 20000

Table 2-6: No-rise condition for the square pier.

Serial No	Bottom channel width (ft)	Flow range (cfs)	Number of piers	Slope (%)	Most upstream cross-section	Immediate bridge upstream cross-section
					Flow (cfs)	Flow (cfs)
1	20	200-5600	2	0.3	Flow ≤ 5600	Flow ≤ 5600
				0.5	Flow ≤ 2600	Flow ≤ 1600
				0.7	Flow ≤ 1800	Flow ≤ 1000
				1	Flow ≤ 1600	Flow ≤ 1000
2	40	200-8400	2	0.3	Flow ≤ 8400	Flow ≤ 8400
				0.5	Flow ≤ 7800	Flow ≤ 6200
				0.7	Flow ≤ 8400	Flow ≤ 5000
				1	Flow ≤ 4200	Flow ≤ 3000
			3	0.3	Flow ≤ 8400	Flow ≤ 8400
				0.5	Flow ≤ 3800	Flow ≤ 2800
				0.7	Flow ≤ 4800	Flow ≤ 2600
				1	Flow ≤ 2600	Flow ≤ 1800
3	60	200-11400	2	0.3	Flow ≤ 11400	Flow ≤ 11400
				0.5	Flow ≤ 11400	Flow ≤ 11400
				0.7	Flow ≤ 9400	Flow ≤ 5800
				1	Flow ≤ 7200	Flow ≤ 4600
			3	0.3	Flow ≤ 11400	Flow ≤ 11400
				0.5	Flow ≤ 8400	Flow ≤ 6400
				0.7	Flow ≤ 6000	Flow ≤ 4600
				1	Flow ≤ 4800	Flow ≤ 2800
4	80	200-13400	2	0.3	Flow ≤ 13400	Flow ≤ 13400
				0.5	Flow ≤ 13400	Flow ≤ 13400
				0.7	Flow ≤ 13400	Flow ≤ 9000
				1	Flow ≤ 8800	Flow ≤ 7200
			3	0.3	Flow ≤ 13400	Flow ≤ 13400
				0.5	Flow ≤ 13400	Flow ≤ 13400
				0.7	Flow ≤ 8200	Flow ≤ 5000
				1	Flow ≤ 7600	Flow ≤ 4800

Serial No	Bottom channel width (ft)	Flow range (cfs)	Number of piers	Slope (%)	Most upstream cross-section	Immediate bridge upstream cross-section
					Flow (cfs)	Flow (cfs)
5	100	200-15000	2	0.3	Flow ≤ 15000	Flow ≤ 15000
				0.5	Flow ≤ 15000	Flow ≤ 15000
				0.7	Flow ≤ 15000	Flow ≤ 13800
				1	Flow ≤ 10400	Flow ≤ 12200
			3	0.3	Flow ≤ 15000	Flow ≤ 15000
				0.5	Flow ≤ 15000	Flow ≤ 15000
				0.7	Flow ≤ 14800	Flow ≤ 11600
				1	Flow ≤ 13600	Flow ≤ 9200
6	120	200-20000	2	0.3	Flow ≤ 20000	Flow ≤ 20000
				0.5	Flow ≤ 20000	Flow ≤ 20000
				0.7	Flow ≤ 20000	Flow ≤ 20000
				1	Flow ≤ 14200	Flow ≤ 19000
			3	0.3	Flow ≤ 20000	Flow ≤ 20000
				0.5	Flow ≤ 20000	Flow ≤ 20000
				0.7	Flow ≤ 20000	Flow ≤ 20000
				1	Flow ≤ 14800	Flow ≤ 13200
7	140	200-20000	3	0.3	Flow ≤ 20000	Flow ≤ 20000
				0.5	Flow ≤ 20000	Flow ≤ 20000
				0.7	Flow ≤ 20000	Flow ≤ 17200
				1	Flow ≤ 15200	Flow ≤ 17600
8	160	200-20000	3	0.3	Flow ≤ 20000	Flow ≤ 20000
				0.5	Flow ≤ 20000	Flow ≤ 20000
				0.7	Flow ≤ 20000	Flow ≤ 20000
				1	Flow ≤ 18200	Flow ≤ 20000
9	180	200-20000	3	0.3	Flow ≤ 20000	Flow ≤ 20000
				0.5	Flow ≤ 20000	Flow ≤ 20000
				0.7	Flow ≤ 20000	Flow ≤ 20000
				1	Flow ≤ 20000	Flow ≤ 20000

Chapter 3. Pier Encasement Effect on Headwater Elevation due to Winter Ice Cover and Ice Jam

Abstract

The bridge pier scours and substructure deterioration due to cold climate has been a serious concern in the United States. The pier encasement is typically undertaken in such cases in order to strengthen the substructure. In cold regions, bridge substructure (pier) can promote the formation of ice jams by hindering the passage of river ice. Moreover, an ice jam formation along the piers can have several adverse effects on river hydraulics and hydrology. This study aims to investigate ice jam effects on headwater elevation after the pile pier encasement. For this, the historical temperature, precipitation and ice jam information was analyzed using a widely accepted hydraulic tool, Hydraulic Engineering Center-River Analysis System (HEC-RAS). A generic cross section was developed in HEC-RAS and the meteorological data required for ice jam analysis was taken from the Northeastern region of Ohio. The hydraulic simulations were carried out for various channel configuration and pier sizes with a wide range of flows to see the effects of pier encasement on headwater elevation. The study showed that the water surface level measured in the upstream cross section of the bridge showed a rise condition, especially for the smaller channel section. The rise condition was detected only for smaller channel bottom width, especially for the higher channel slope and higher flow rate. While ice jam conditions increased the water surface elevation, the pier encasement did not significantly contribute to additional increase in water surface elevation

Keywords: Pier, Ice Jam, water surface elevation

Introduction

As discussed earlier, the bridges initial design and their maintenance have constantly been a significant challenge for engineers and constructors over the time. Typically, bridges are designed for a 100-year period but may encounter several hazards in terms of flooding, ice jam and other unanticipated loads within this period. Therefore, routine maintenance and rehabilitation of the bridges are essential. Pier encasement is a rehabilitation method often used to allow the reuse of existing pile piers during the repair, rehabilitation or replacement of the bridge structure. The bridge rehabilitation projects involve a deck replacement with the pier encasement as an element of the repair. In cold region during winter, bridge structures are heavily affected by river ice. The structural component like piers directly experiences the horizontal and vertical forces exerted by river ice. The accumulation of broken ice leads to buckling of superstructures; scouring of channel bed due to the release of ice jam waves; and various effects of vibration on lanky structures (AASHTO 2002; Neill 1981; RTAC 1981). It is one of the most vital hydraulic stress to the bridge structures in cold region during winter. Ice jams are considered fatal than open-water floods (Beltaos and Burrell, 2002). Ice jam provides an additional solid boundary to the flowing water affecting the flow velocity. Moreover, the presence of bridge pier further changes the flow conditions around the bridge piers. Thus affecting the accumulation of ice jam near bridge pier (W. A. N. G. et al., 2015). Few previous studies suggest that pier triggers the formation of the ice jam, and thus increases the possibility of ice jam flooding (Beltaos, 2008; Beltaos, 2007). The moving ice gets packed up slowly in the downstream and forms an arch between bridge piers (Urroz et al., 1994). More importantly, ice strikes a pier creating dynamic forces depending upon the geometry of pier, strength, and size of the ice (Montgomery and Gerard, 1980). Ice covers and ice jams increase the wetted perimeter and flow resistance provided by shear force at the underside of an ice cover leading to the increase in water surface elevation (Zufelt et al., 2006). Earlier studies reported that a 10-year frequency ice jam flood can attain flood levels greater than that of a 100-year event for open water conditions (Gary et al., 2003). Therefore, even for the limited flow, the ice jam results into a very high water levels causing more ice-related bridge damages. Moreover, the ice levels and ice movement can impair bridges and other infrastructure along the river. The four types of jam-prone sites have been identified: channel constriction, a decrease in river slope, sharp bend, and shallow stream allowing ice to ground (Shattuck, 1988).

The majority of the rivers in the northern side of USA experiences ice jams causing significant flooding, infrastructure damage, hindrance in navigation and affecting the environment (Beltaos and Prowse, 2009; Tuthill, 2000; Carr and Tuthill, 2011; Vuyovich et al, 2009). There are numerous such instances where bridge destruction and failure occurred due to ice jam (Beltaos et al., 2007).

Since the effect of pier encasement was explored on head water elevation during no-ice conditions in the earlier chapter, I wanted to see the effect of pier encasement on ice jam conditions near the bridges, which is very common especially in the northern belt of USA. While there has been a number of research conducted regarding ice jam and resulting flood near the bridge sites (Beltaos et al., 2006), the additional effect of pier encasement on headwater elevation due to winter ice cover and ice jam has never been studied before. Moreover, there are very less documented literature on the potential impact of ice jam after bridge pier encasement. Therefore, the major objective of this paper is to investigate the effect of winter ice cover/ice jam on water surface elevation within the bridge vicinity after the pier encasement.

Theoretical Descriptions

The Hydrologic Engineering Centers River Analysis System (HEC-RAS), a hydraulic modeling software, was used to study the effect of ice cover and an ice jam on water surface elevation around the bridge vicinity. The chapter 2 of the thesis discusses the detail theoretical description of HEC-RAS.

The ice jam modeled through HEC-RAS commonly falls under the category of wide-river ice jams (Gary et al., 2003). HEC-RAS permits the users to simulate wide-river jams or model ice-covered channels with known ice properties (Daly et al., 1998). To simulate wide-river jams, it solves both energy and force balance equation in each cross section and determines the ice thickness. Users can specify the ice cover roughness and thickness values at every cross section to model the ice jam. Both these values can vary along the channel. Force balance is used in the downstream direction and energy equation is in the upstream direction employing the process of iteration to find the solution. In the first step, the ice thickness is estimated and water surface profile is computed from the upstream using the energy equation. In the next step, ice thickness is recalculated for all cross section by using a force balance equation from the upstream end. The use of energy and force balance equation continues until the ice thicknesses and water surface elevation computed by both the methods converge. Brunner (2010) gave the equations involved in ice jam simulation process as follows.

$$\frac{dt}{dx}=\frac{1}{2k_p\gamma}\left[\rho g S_w+\frac{\tau}{t}\right]-\frac{k_0 k_1}{B}t=F \qquad (3.1)$$

Where F implies the force balance equation, t is accumulation thickness, x is longitudinal distance, ρ is density of ice, S_w is water surface slope, τ is shear stress applied beneath the ice by the flowing water, g is acceleration due to gravity, k_1 is the ratio of lateral to longitudinal pressure, B is accumulation width.

Ice jam can be estimated in the river using the accumulated freezing degree-days (AFFD), which can be estimated by using the average daily air temperature. AFDD is an indicator of winter severity, which is computed by accumulating freezing degree days (FDD) from the beginning of winter season. Where FDD is usually computed as a sum of average daily air temperatures when it is below freezing for a stated time. Following is Stefan's equation to estimate the ice thickness based on AFDD.

$$t_f = c\sqrt{AFDD} \tag{3.2}$$

$$AFDD = (32 - T_o) \tag{3.3}$$

Where AFDD is Accumulated Freezing Degree Days and T_o is the daily average air temperature in ^{0}F; T_f is the ice thickness in inches, c is a coefficient for ice cover conditions, including wind exposure and snow cover. For a small sheltered river, an average value of c is 0.30 (USACE, 2002). Table 3-1 lists various values of coefficient "c" for different environmental conditions.

Based on the ice thickness provided at the upstream, typically the downstream ice thickness is computed using a force balance equation, which is similar to standard step method. Brunner (2010) gave the following equations to calculate downstream ice thickness.

$$\overline{\mathrm{F}} = \frac{T_{\mathrm{ds}} - T_{\mathrm{us}}}{\mathrm{L}} \tag{3.4}$$

$$\overline{\mathrm{F}} = \frac{f_{us} + f_{ds}}{2} \tag{3.5}$$

Where T_{us} is a thickness at the upstream section and T_{ds} is a thickness at the downstream section and L is the distance between two cross sections. Similarly, the ice jam forces at upstream and downstream are $\mathrm{f_{us}}$ and $\mathrm{f_{ds}}$, respectively. The computed ice jam thickness cannot be lower than the provided thickness. If less, the provided thickness is taken.

Materials and Methodology

Study Area

This study was also conducted using generic channel section; therefore, no specific study area location has been described. However, for simulation of an ice jam in HEC-RAS, it requires ice thickness, which was estimated based on the temperature data of one of the NCDC stations located near the Grand River of the Northeastern region of Ohio. Over the past few decades, Grand River has been frequently experiencing ice jam in numerous sections along the river channel.

Bridge Pier Encasement

The types of pier used and basic approach employed for the encasement has been discussed in chapter 2 under the heading "Bridge Pier Encasement".

Overall Modeling Approach

Hydraulic Engineering Center's River Analysis System (HEC-RAS) developed by the US Army Corps of Engineers has been used for performing one-dimensional hydraulic computation (Daly et al., 2003). Modeling the ice-covered channels of known thickness and roughness or ice jam simulations can be done in HEC-RAS (Daly et al., 1998). Nevertheless, the manual input of ice jam locations must be specified as HEC-RAS cannot recognize the ice jam location in the river (Brunner, 2010). The general details of modeling approach employed in the study are described in chapter 2 under heading “Overall Modeling Approach”. However, ice jam modeling approach has been explained in the following paragraph.

In order to estimate the ice thickness, first, we estimated the AFDD of each year for the winter period starting from 1949 to 2013. Furthermore, the estimated AFDD was used to compute ice thickness by using modified Stefan’s equation. For the hydraulic analysis, the maximum possible thickness of ice cover in the Grand River was taken based on the historical data. Moreover, the Nezhikovsky’s (1964) equation was used to find out the hydraulic roughness of an ice jam. The roughness value was provided in the section where ice jam scenario was applied. The value adopted for manning’s roughness was 0.025. For the simulation of the ice jam, HEC-RAS also requires a separate set of manning’s roughness for channel and floodplain, the roughness value for channel section was adopted as 0.035 and 0.15 for flood plains (Lamichhane, 2016). In order to run the model in HEC-RAS, the estimated ice thickness was provided at each cross section. The program was run for two different cases: a) simulation with ice jam but without pier encasement (existing); b) simulation with ice jam after pier encasement (proposed). The water surface elevation in bridge vicinity was compared for two different simulations.

HEC-RAS Model Inputs

The entire model input (channel properties, discharge, the number of the pier, type of encasement etc.) has been already described under heading "HEC-RAS Model Input" in chapter 2. The ice thickness and roughness value were additionally incorporated to explore the impact of an ice jam on bridges with pier encasement. The other necessary data required for ice simulation like ice jam porosity, the ratio of lateral to longitudinal pressure (k_1), maximum mean velocity under ice cover, internal friction angle of jam, ice cohesion were chosen as a default value from HEC-RAS, which are presented in Table 3-2. Moreover, the ice jam location was entered manually in the river cross-section.

Model Establishment

The same model was used for this study as well. The details of model establishment using HEC-RAS has been already described in chapter 2.

Results

AFDD and Ice Thickness Calculations

The accumulated freezing degree days (AFDD) was computed by summing up the freezing degree days (FDD). The AFDD value increased with the decrease in temperature. The historical temperature data for the period of 1949 to 2013 was used to calculate the ice thickness. By using Stefan's equation 3.2 with a coefficient value of 0.3, the maximum AFDD of 1068-degree produced a 10-inch thick ice cover for the period 1977-1978. HEC-RAS used this maximum thickness value to simulate winter discharge and to compute the effect of ice cover and an ice jam on water surface elevation in bridge vicinity before and after the pier encasement.

Ice Jam Impact on WSE after Encasement.

The water surface elevation produced at bridge upstream and immediate bridge upstream were compared for existing and proposed pier condition. As discussed in chapter 2, the rise and no rise condition were classified depending upon the allowable surcharge limit of flood set for Ohio. The analysis indicates that the result was consistent with the results obtained in Chapter 2.

The no-rise condition obtained after running ice jam simulation for existing and proposed pier was tabulated in Table 3-3. The range of flow was selected based on the flow accommodating capacity of the channel. For example, a 20 ft. channel bottom width with a slope of 0.3% and 0.5% showed no-rise condition for flow range up to 5600 cfs. Relatively for higher slope like 0.7% and 1%, the rise condition was realized. For example, rise condition would be experienced after 3000 cfs and 1800 cfs, for 0.7% and 0.1% slope, respectively. The detail ranges of the flows for a no-rise condition for various channel configurations has been reported in Table 3-3. Any values exceeding the flow ranges (as reported in Table 3-3) for the respective channel configurations would produce the rise condition. Similarly, Table 3-4 depicted a no-rise in water surface elevation for square piers using two and three piers for all the channel configurations.

The channel's bottom width had a considerable effect on water surface elevation compared to other channel configurations and properties. For example, the difference in water surface elevation for existing and proposed pier for the channel section of 20 ft bottom width with 1.0% channel slope and 5000 cfs flow showed a greater rise in water surface elevation (0.90 ft). However, for a channel of 180 ft bottom width with the same channel section properties and same flow (5000 cfs), the rise in water surface elevation was comparatively less (0.01 ft).

The effect of flow volume was not crucial in the case of a channel with ice jam. For example, the difference in water surface elevation for existing and proposed pier for the channel section of 20 ft with 1.0% slope, the rise in water surface elevation was much lesser for 200 cfs (0.08 ft) when compared to flow volume 5000 cfs (0.90 ft) (not shown). Whereas, in the wider channel, even the higher flow had no considerable difference in headwater elevation. For example, the difference in water surface elevation for an existing and proposed pier for the channel section of 100 ft with 1.0% slope, the rise in water surface elevation was much lesser for 200 cfs (no change) when compared to flow volume 5000 cfs (0.04 ft) (not shown). This pattern was true even for higher channel slope indicating that slope did not have significant effect to increase the water surface elevation, especially for the wider channel.

The difference in water surface elevation for 20 ft, 100 ft and 180 ft were plotted against the flow for all the four slopes 0.3%, 0.5%, 0.7% and 1.0%. Figure 3-1 shows the plot for 20 ft channel width at most bridge upstream cross section with two circular piers. The channel section with 0.3% and 0.5% showed no rise for all the possible flow ranges. With the increase in slope, rise condition started to appear. For example, the rise condition was detected after 3000 cfs for 0.7% slope, whereas the rise condition was observed soon after 1800 cfs for 1% slope. Figure 3-2 shows the plot for immediate bridge upstream cross section for the 20 ft channel section. A similar trend was detected with 0.3% and 0.5%

showing no rise for all the possible flow ranges. However, it started gradually increasing as the slope was increased. For example, the rise condition appeared for 0.7% slope at flows greater than 1200 cfs, whereas the rise condition was observed after 400 cfs for 1.0% slope.

Figure 3-3 and Figure 3-4 show the difference in water surface elevation at most bridge upstream and immediate bridge upstream for all the flows (200 cfs - 15000 cfs), for channel section of 100 ft bottom width with two circular piers. For all the flow ranges, it showed a no-rise condition in both the cross section. Similarly, Figure 3-5 and Figure 3-6 shows the difference in water surface elevation at most bridge upstream and immediate bridge upstream for all the flows (200 cfs - 20000 cfs), for channel section of 180 ft bottom width with two circular piers. For all the flow ranges, it showed a no-rise condition in both the cross sections.

The analysis indicated that the difference in water surface elevation after the encasement decreased with an increase in channel bottom width. As we discussed in the earlier chapter, increased slope and higher flow volume produced a greater rise in water surface elevation after the encasement. However, its effect was limited only to smaller channel bottom width. Nevertheless, its effect was negligible in wider channel width. Typically, the rise condition was prevalent only in narrow channel bottom width. After analyzing both in no-ice conditions (chapter 2), and ice conditions (this chapter), it is interesting to report that ice jam does not have any additional effect on rise in water surface elevation. While ice jam was always crucial to increase the headwater elevation, the increase in water surface elevation did not arise due to the encasement but it was created due to the jam itself as the increase in water surface elevation was very nominal compared to what was obtained in chapter 2.

Conclusions

The ice jam formation and its growth can have a vital effect on engineering structures, especially in cold regions. The bridge pier enhances the process of ice jamming and has an effect on flow hydraulics. Since the effect of pier encasement on water surface elevation in bridge vicinity is still unknown to us, the aim of this study was to document the effect of pile pier encasement under varying model conditions to determine the rise in water surface elevation at bridge upstream. This study of the effect of an ice jam at bridge location based on changes in water surface elevation was carried out in HEC-RAS. Each channel in the study was modeled for four channel slopes (0.3%, 0.5%, 0.7% and 1.0%). Moreover, for every channel configuration, two separate models were developed: one without pier encasement (existing); and other with pier encasement (proposed).

Furthermore, the difference of water surface elevation for existing and proposed pier configuration was computed for all the channel sections. The computed difference was broadly categorized into the rise and no-rise conditions depending upon the simulated water level in the upstream section of the bridge. The rise and no-rise condition were declared as per Ohio standards, which considers the no-rise condition if the increased water surface elevation was limited to 0.5 ft.

Finally, it was found out that, the increase in water surface elevation after pier encasement was a function of channel bottom width. In addition, the other factors as channel slope and flow volume made a very little difference in water surface elevation.

The constriction of the channel is one of the main reason for the increase in water surface elevation. With encasement, pier width increased constricting the channel more and magnifying the effect. The difference was visible for smaller channel width, especially with higher channel slopes and flow volume. However, with the widening of channel section, there was a sharp decrease in the difference in water surface elevation between the encased and non-encased case. Even with higher slopes and flow volume, the rise condition was hard to achieve for wider channel width.

After analyzing with ice jam conditions, it was clear that pier encasement effect to raise in water surface elevation was not crucial at all in ice jam conditions. While ice jam condition increased the water surface elevation, there was not any considerable difference in water surface elevation regardless of pier encasement or no pier encasement.

References:

AASHTO. (2002). “Standard specifications for highway bridges.” American Association of State Highway and Transportation Officials Report Code HB-17, Washington, D.C.

Beltaos, Spyros. "Progress in the study and management of river ice jams." Cold Regions Science and Technology 51.1 (2008): 2-19.

Beltaos, Spyros, et al. "Hydraulic effects of ice breakup on bridges. “Canadian Journal of Civil Engineering 34.4 (2007): 539-548.

Beltaos, Spyros, et al. "Formation of breakup ice jams at bridges." Journal of Hydraulic Engineering 132.11 (2006): 1229-1236.

Beltaos, Spyros, and Brian C. Burrell. "Extreme ice jam floods along the Saint John River, New Brunswick, Canada." IAHS Publication (2002): 9-14.

Beltaos, Spyros, and Terry Prowse. "River-ice hydrology in a shrinking cryosphere." Hydrological Processes 23.1 (2009): 122-144.

Brunner, Gary W. HEC-RAS River Analysis System. Hydraulic Reference Manual. Version 4.1. Hydrologic Engineering Center Davis CA, 2010

Carr, Meredith L., and Carrie M. Vuyovich. "Investigating the effects of long-term hydro-climatic trends on Midwest ice jam events." Cold Regions Science and Technology 106 (2014): 66-81.

Carr, Meredith L., and Andrew M. Tuthill. "Modeling of scour-inducing ice effects at Melvin Price Lock and Dam." Journal of Hydraulic Engineering 138.1 (2011): 85-92.

Daly, Steven F., et al. "Modeling ice-covered rivers using HEC-RAS." Cold Regions Impact on Civil Works: ASCE, 1998.

Dyhouse, Gary, et al. "Floodplain modeling using HEC-RAS." (2003).

Hopkins, M. A., and Steven F. Daly. "Recent advances in discrete element modeling of river ice." Proceedings, 12th workshop on the Hydraulics of ice covered rivers. 2003.

Jun, W. A. N. G., et al. "Impact of bridge pier on the stability of ice jam." Journal of Hydrodynamics, Ser. B 27.6 (2015): 865-871.s

Lamichhane, Niraj. Prediction of Travel Time and Development of Flood Inundation Maps for Flood Warning System Including Ice Jam Scenario. A Case Study of the Grand River, Ohio. Diss. Youngstown State University, 2016.

Montgomery, C. James, Robert Gerard, and A. William Lipsett. "Dynamic response of bridge piers to ice forces." Canadian Journal of Civil Engineering 7.2 (1980): 345-356.

Neill, C. R. "Ice effects on bridges." Roads and Transportation Association of Canadá, Ottawa, Ontario, Canadá (1981).

Roads and Transportation Association of Canada (RTAC). (1981). Ice effects on bridges, C. R. Neill, ed., Ottawa, Canada.

Shattuck, Robert F. Ice jams at highways and Bridges-causes and Remedial Measures. No. HS-038 995. 1984.

Tuthill, A. M. "Managing ice at Corps of Engineers locks and dams: Current solutions and future needs." Proc., 15th IAHR Symp. on Ice. Vol. 2. Delft, The Netherlands: International Association of Hydraulic Research and Engineering, 2000.

Urroz, Gilberto E., Joseph Schaefer, and Robert Ettema. "Bridge-pier location and ice conveyance in curved channels." Journal of cold regions engineering 8.2 (1994): 66-72.

USACE, US. "Army Corps of Engineers 2003." Coastal Engineering Manual, Part. V. Coastal and Hydraulics Lab., US Army Engineer Research and Development Center, Vicksburg, Mississippi, USA (2002).

Vuyovich, Carrie M., Andrew M. Tuthill, and John J. Gagnon. Physical Model Study of Cross Vanes and Ice. No. ERDC/CRREL TR-09-7. Engineer Research and Development Center Hanover NH Cold Regions Research and Engineering Lab, 2009.

White, Kathleen D., Andrew M. Tuthill, and Linnzi Furman. "Studies of ice jam flooding in the United States." Extreme Hydrological Events: New Concepts for Security. Springer Netherlands, 2006. 255-268.

White, K. (2004). Method to estimate river ice thickness based on meteorological data: ERDC. CRREL Technical Note TN-04-3, US Army Engineer Research and Development Center, Hanover, New Hampshire.

Zufelt, Jon E., Carrie M. Vuyovich, and Timothy B. Baldwin. "Modeling of Aufeis-Induced Flooding." Current Practices in Cold Regions Engineering. 2006. 1-13.Hara, F., S. Kunimatsu, and H. Saeki. "Conditions of arch formation by ice floes at bridge piers." Proc., 12th Ice Symp. Vol. 2. 1994.

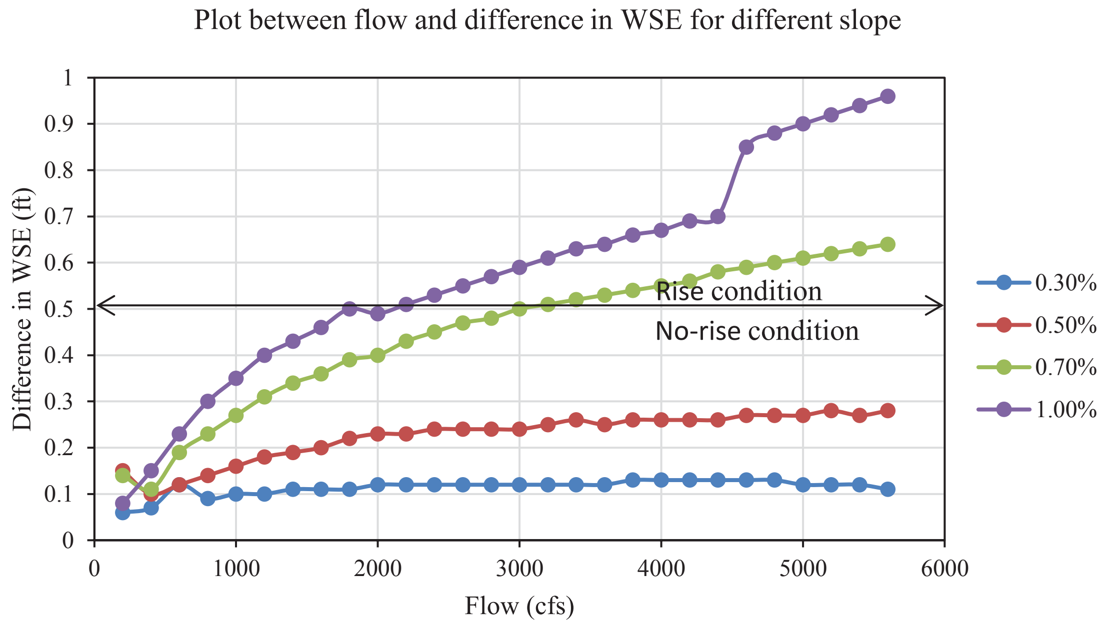

Figure 3-1: The difference in WSE at most upstream for 20 ft channel section.

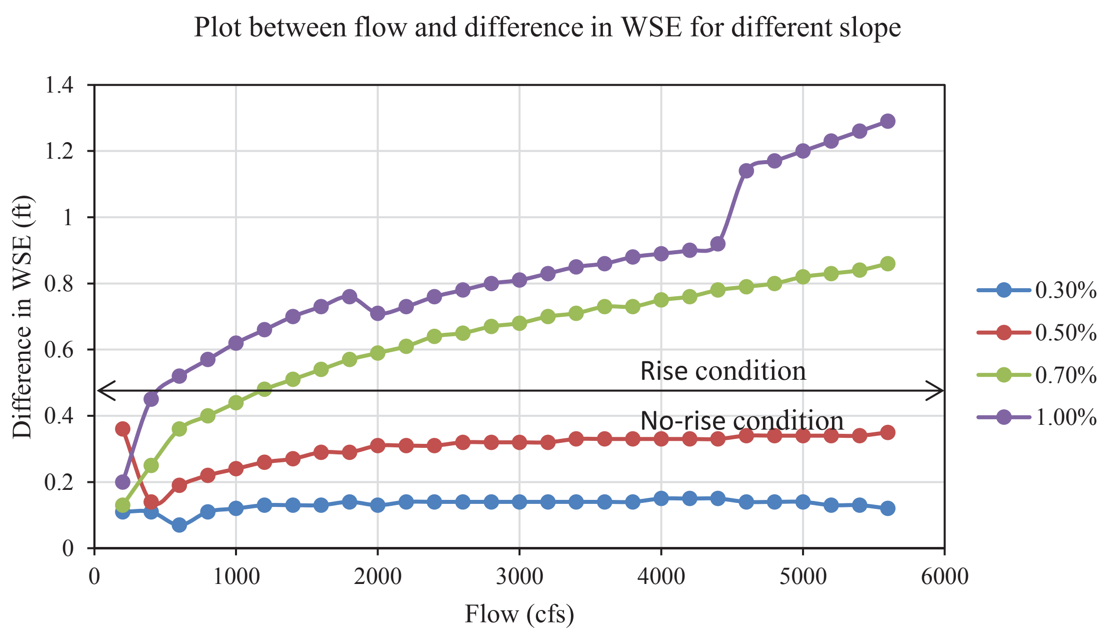

Figure 3-2: The difference in WSE at immediate upstream for 20 ft channel section.

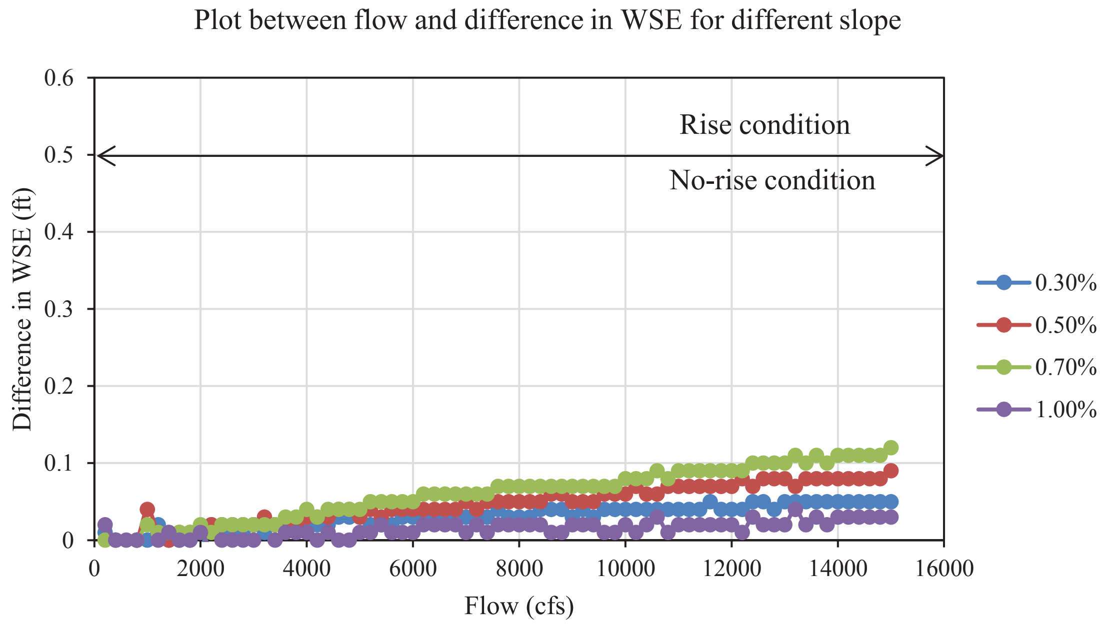

Figure 3-3: The difference in WSE at most upstream for 100 ft channel.

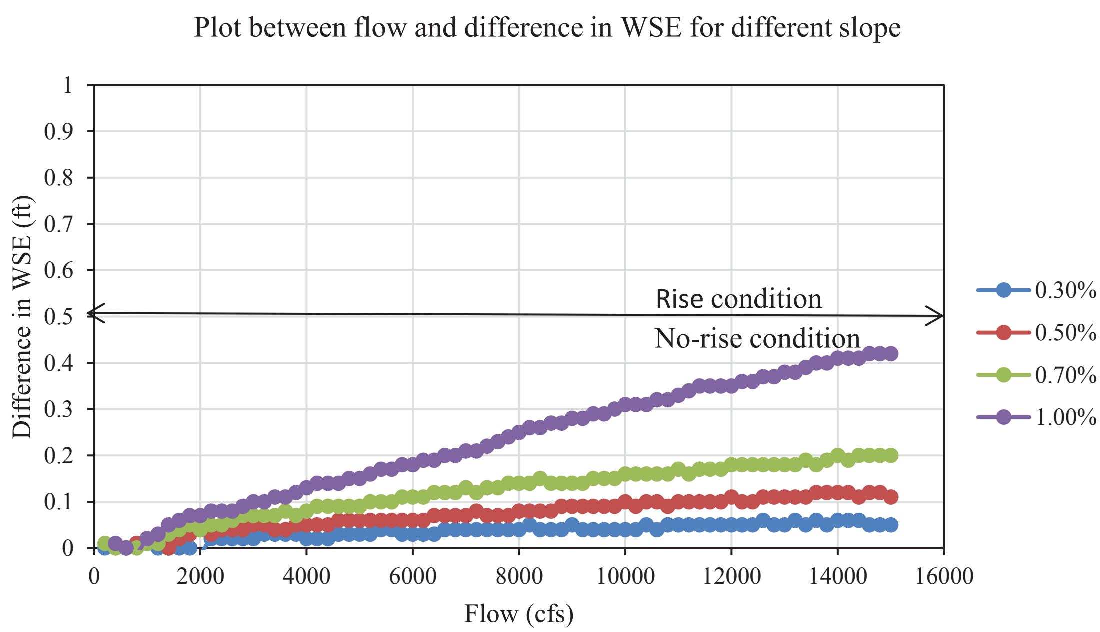

Figure 3-4: The difference in WSE at immediate upstream for 100 ft channel section.

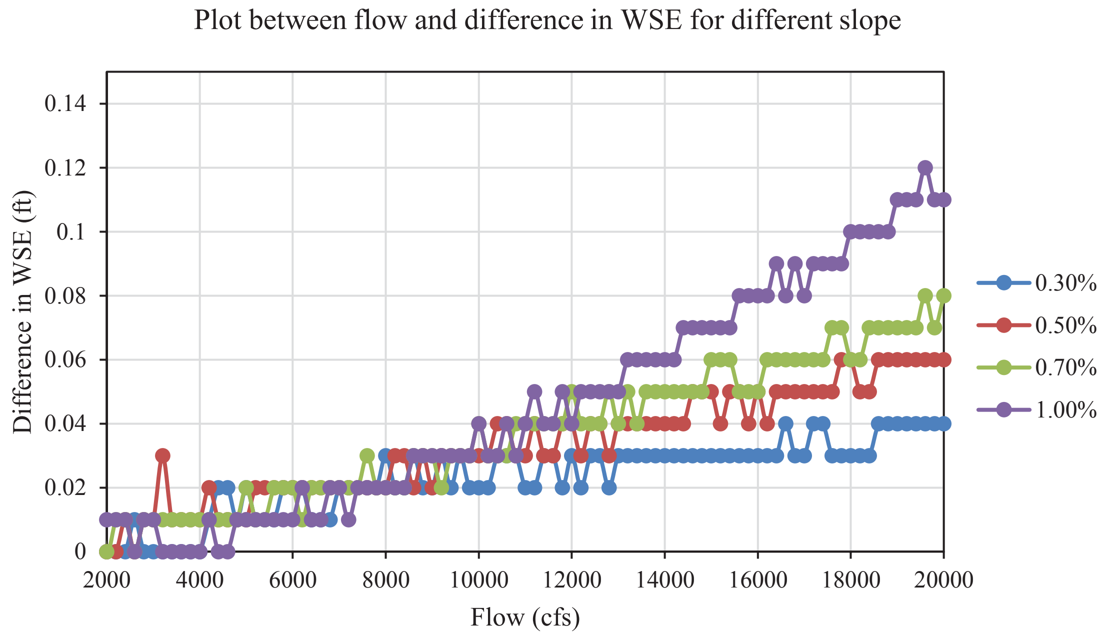

Figure 3-5: The difference in WSE at most upstream for 180 ft channel section.

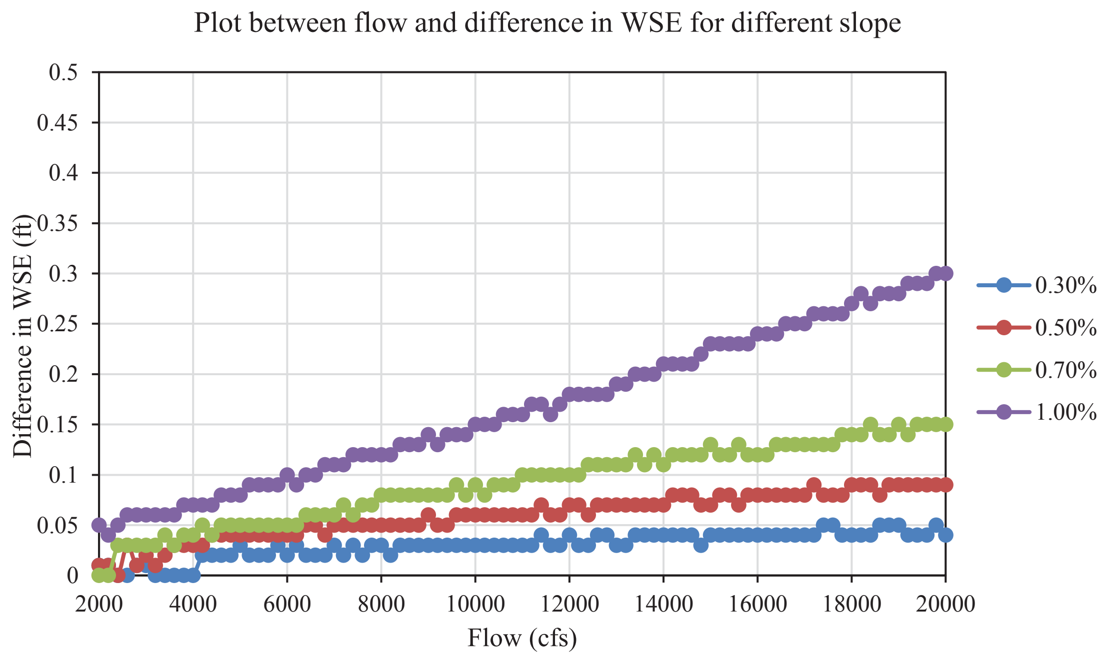

Figure 3-6: The difference in WSE at immediate for 180 ft channel section.

Table 3-1: c values for different conditions taken from USACE, 2002

Serial No	Condition	c (when AFDD is calculated using degree Fahrenheit)
1	Windy lake with no snow	0.8
2	Average lake with snow	0.5 – 0.7
3	Average river with snow	0.4 – 0.5
4	Sheltered small river with rapid flow	0.2 – 0.4

Table 3-2: HEC-RAS default ice jam parameters

Parameter	Value	Parameters	Value
Angle of internal friction	45^0	Ice cohesion	0
Ratio of lateral to longitudinal pressure (k1)	0.33	Maximum flow value under the jam	5 fps
Density of ice	0.916	Jam porosity	0.4

Table 3-3: No-rise condition for the circular pier.

Serial No	Bottom channel width (ft)	Flow range (cfs)	Number of piers	Slope (%)	Most upstream cross-section	Immediate bridge upstream cross-section
					Flow (cfs)	Flow (cfs)
1	20	200-5600	2	0.3	Flow ≤ 5600	Flow ≤ 5600
				0.5	Flow ≤ 5600	Flow ≤ 5600
				0.7	Flow ≤ 3000	Flow ≤ 1200
				1	Flow ≤ 1800	Flow ≤ 400
2	40	200-8400	2	0.3	Flow ≤ 8400	Flow ≤ 8400
				0.5	Flow ≤ 8400	Flow ≤ 8400
				0.7	Flow ≤ 8400	Flow ≤ 8400
				1	Flow ≤ 6000	Flow ≤ 2400
			3	0.3	Flow ≤ 8400	Flow ≤ 8400
				0.5	Flow ≤ 8400	Flow ≤ 8400
				0.7	Flow ≤ 6800	Flow ≤ 4000
				1	Flow ≤ 2400	Flow ≤ 800
3	60	200-11400	2	0.3	Flow ≤ 11400	Flow ≤ 11400
				0.5	Flow ≤ 11400	Flow ≤ 11400
				0.7	Flow ≤ 11400	Flow ≤ 11400
				1	Flow ≤ 11400	Flow ≤ 5600
			3	0.3	Flow ≤ 11400	Flow ≤ 11400
				0.5	Flow ≤ 11400	Flow ≤ 11400
				0.7	Flow ≤ 11400	Flow ≤ 7800
				1	Flow ≤ 6400	Flow ≤ 2400
4	80	200-13400	2	0.3	Flow ≤ 13400	Flow ≤ 13400
				0.5	Flow ≤ 13400	Flow ≤ 13400
				0.7	Flow ≤ 13400	Flow ≤ 13400
				1	Flow ≤ 13400	Flow ≤ 12000
			3	0.3	Flow ≤ 13400	Flow ≤ 13400
				0.5	Flow ≤ 13400	Flow ≤ 13400
				0.7	Flow ≤ 13400	Flow ≤ 13400
				1	Flow ≤ 9200	Flow ≤ 6200

Serial No	Bottom channel width (ft)	Flow range (cfs)	Number of piers	Slope (%)	Most upstream cross-section	Immediate bridge upstream cross-section
					Flow (cfs)	Flow (cfs)
5	100	200-15000	2	0.3	Flow ≤ 15000	Flow ≤ 15000
				0.5	Flow ≤ 15000	Flow ≤ 15000
				0.7	Flow ≤ 15000	Flow ≤ 15000
				1	Flow ≤ 15000	Flow ≤ 15000
			3	0.3	Flow ≤ 15000	Flow ≤ 15000
				0.5	Flow ≤ 15000	Flow ≤ 15000
				0.7	Flow ≤ 15000	Flow ≤ 15000
				1	Flow ≤ 14000	Flow ≤ 9400
6	120	200-20000	2	0.3	Flow ≤ 20000	Flow ≤ 20000
				0.5	Flow ≤ 20000	Flow ≤ 20000
				0.7	Flow ≤ 20000	Flow ≤ 20000
				1	Flow ≤ 20000	Flow ≤ 20000
			3	0.3	Flow ≤ 20000	Flow ≤ 20000
				0.5	Flow ≤ 20000	Flow ≤ 20000
				0.7	Flow ≤ 20000	Flow ≤ 20000
				1	Flow ≤ 20000	Flow ≤ 13800
7	140	200-20000	3	0.3	Flow ≤ 20000	Flow ≤ 20000
				0.5	Flow ≤ 20000	Flow ≤ 20000
				0.7	Flow ≤ 20000	Flow ≤ 19000
				1	Flow ≤ 20000	Flow ≤ 19200
8	160	200-20000	3	0.3	Flow ≤ 20000	Flow ≤ 20000
				0.5	Flow ≤ 20000	Flow ≤ 20000
				0.7	Flow ≤ 20000	Flow ≤ 20000
				1	Flow ≤ 20000	Flow ≤ 20000
9	180	200-20000	3	0.3	Flow ≤ 20000	Flow ≤ 20000
				0.5	Flow ≤ 20000	Flow ≤ 20000
				0.7	Flow ≤ 20000	Flow ≤ 20000
				1	Flow ≤ 20000	Flow ≤ 20000

Table 3-4: No-rise condition for the square pier.

Serial No	Bottom channel width (ft)	Flow range (cfs)	Number of piers	Slope (%)	Most upstream cross-section	Immediate bridge upstream cross-section
					Flow (cfs)	Flow (cfs)
1	20	200-5600	2	0.3	Flow ≤ 5600	Flow ≤ 5600
				0.5	Flow ≤ 5600	Flow ≤ 5600
				0.7	Flow ≤ 5600	Flow ≤ 5600
				1	Flow ≤ 1800	Flow ≤ 600
2	40	200-8400	2	0.3	Flow ≤ 8400	Flow ≤ 8400
				0.5	Flow ≤ 8400	Flow ≤ 8400
				0.7	Flow ≤ 8400	Flow ≤ 8400
				1	Flow ≤ 5800	Flow ≤ 2400
			3	0.3	Flow ≤ 8400	Flow ≤ 8400
				0.5	Flow ≤ 8400	Flow ≤ 8400
				0.7	Flow ≤ 5000	Flow ≤ 7600
				1	Flow ≤ 2800	Flow ≤ 1000
3	60	200-11400	2	0.3	Flow ≤ 11400	Flow ≤ 11400
				0.5	Flow ≤ 11400	Flow ≤ 11400
				0.7	Flow ≤ 11400	Flow ≤ 11400
				1	Flow ≤ 11400	Flow ≤ 7200
			3	0.3	Flow ≤ 11400	Flow ≤ 11400
				0.5	Flow ≤ 11400	Flow ≤ 11400
				0.7	Flow ≤ 11400	Flow ≤ 11400
				1	Flow ≤ 6600	Flow ≤4000
4	80	200-13400	2	0.3	Flow ≤ 13400	Flow ≤ 13400
				0.5	Flow ≤ 13400	Flow ≤ 13400
				0.7	Flow ≤ 13400	Flow ≤ 13400
				1	Flow ≤ 13400	Flow ≤ 13400
			3	0.3	Flow ≤ 13400	Flow ≤ 13400
				0.5	Flow ≤ 13400	Flow ≤ 13400
				0.7	Flow ≤ 13400	Flow ≤ 13400
				1	Flow ≤ 12200	Flow ≤ 10600

Serial No	Bottom channel width (ft)	Flow range (cfs)	Number of piers	Slope (%)	Most upstream cross-section	Immediate bridge upstream cross-section
					Flow (cfs)	Flow (cfs)
5	100	200-15000	2	0.3	Flow ≤ 15000	Flow ≤ 15000
				0.5	Flow ≤ 15000	Flow ≤ 15000
				0.7	Flow ≤ 15000	Flow ≤ 15000
				1	Flow ≤ 15000	Flow ≤ 15000
			3	0.3	Flow ≤ 15000	Flow ≤ 15000
				0.5	Flow ≤ 15000	Flow ≤ 15000
				0.7	Flow ≤ 15000	Flow ≤ 15000
				1	Flow ≤ 15000	Flow ≤ 12800
6	120	200-20000	2	0.3	Flow ≤ 20000	Flow ≤ 20000
				0.5	Flow ≤ 20000	Flow ≤ 20000
				0.7	Flow ≤ 20000	Flow ≤ 20000
				1	Flow ≤ 20000	Flow ≤ 20000
			3	0.3	Flow ≤ 20000	Flow ≤ 20000
				0.5	Flow ≤ 20000	Flow ≤ 20000
				0.7	Flow ≤ 20000	Flow ≤ 20000
				1	Flow ≤15000	Flow ≤13800
7	140	200-20000	3	0.3	Flow ≤ 20000	Flow ≤ 20000
				0.5	Flow ≤ 20000	Flow ≤ 20000
				0.7	Flow ≤ 20000	Flow ≤ 17200
				1	Flow ≤ 15400	Flow ≤ 17800
8	160	200-20000	3	0.3	Flow ≤ 20000	Flow ≤ 20000
				0.5	Flow ≤ 20000	Flow ≤ 20000
				0.7	Flow ≤ 20000	Flow ≤ 20000
				1	Flow ≤ 20000	Flow ≤ 20000
9	180	200-20000	3	0.3	Flow ≤ 20000	Flow ≤ 20000
				0.5	Flow ≤ 20000	Flow ≤ 20000
				0.7	Flow ≤ 20000	Flow ≤ 20000
				1	Flow ≤ 20000	Flow ≤ 20000

Chapter 4. Effect of Pier Encasement on Headwater Elevation in Grand River Using HEC-RAS Model

Abstract

As discussed in the previous chapters, even the minimal work within the waterway can have a significant effect on the water surface elevation leading to a disastrous flooding, especially in high-risk flood zones. The earlier analysis was conducted using a generic channel section with hypothetical data. Therefore, in this chapter, the result obtained from the previous analysis is validated with the real world application by further testing in the Grand River of Northeastern Ohio. The process of pier encasement was carried out on four bridges of the Grand River. Consequently, the model was prepared and simulated in Hydraulic Engineering Center-River Analysis System (HEC-RAS) for two scenarios (with ice jam and without ice jam). The study showed that the water surface elevation measured in the upstream cross section of the bridge after the encasement exhibited no-rise condition. The maximum rise of 0.04 ft was attained in the case of the channel without ice jam. However, for the channel with ice jam, the maximum rise of 0.03 ft was reached. This meager rise was also experienced in a smaller channel width (134 ft and 147 ft). Conversely, for relatively bigger channel width like 213 ft and 251 ft, there was no change in water surface elevation even after the encasement for both the scenario. The result obtained from this application is consistent with the result discussed in the earlier chapters using hypothetical generic channel sections.

Introduction

The findings obtained from the analysis in previous chapters is further tested in Grand River, OH. The objective of this study was to examine the changes in water surface elevation at the bridge upstream for the encased and non-encased pier at Grand River, OH both in ice-jam and no-ice jam conditions. In order to conduct this analysis, HEC-RAS model was used and the pier encasement effect on water surface elevation was investigated.

Material and Methodology

Study Area

The study was undertaken in Grand River watershed located in the Northeastern region of Ohio. The major stream includes the Grand River (102.7 miles), Mill Creek (28.8 miles), Rock Creek (18.4 miles), and Big Creek (15.6 miles). The watershed has an area of 712 square miles. The Grand River arises from expansive wetlands in southeastern Geauga County, and before emptying into Lake Erie at Painesville, it passes through counties like Trumbull, Ashtabula, Portage and Lake County. The river section of approximately 32.2 miles from Harpersfield to Fairport Harbor was considered as a study site to perform the hydraulic analysis.

Bridge Pier Encasement

The pier encasement was considered in bridges located in Mill creek and Paine creek for the hydraulic analysis. There were altogether four bridges in the Grand River. Each pier in the bridge was encased which increased its width by 2 feet. The hydraulic simulation was run for encased and non-encased condition and the difference in water surface elevation was reported.

Modeling Approach

The analysis was performed using the HEC-RAS model developed on the Grand River by Niraj Lamichhane (Lamichhane, 2016). Figure 4-1 below shows the hydraulic model of Grand River with bridge station in HEC-RAS. Two separate simulations were carried out for the non-encased and encased conditions and the generated water surface elevation was compared.

Lamichhane (2016) developed the hydraulic model by integrating very high-resolution data (LiDAR) in flood plain with actual field survey data of the river channel. Readers can refer the article (Lamichhane and Sharma, 2017) for the detailed methodology of HEC-RAS model development in the Grand River using LiDAR and field survey data.

Results and discussions

The water surface elevation generated at the upstream cross section of the bridges located on the Grand River was studied for existing and proposed pier encasement. The comparison was done for both scenarios. It was found that the difference in water surface elevation for both scenarios was identical with the previously conducted parametric study in chapter 2 & 3. Table 4-1 below shows the difference in water surface elevation generated at the immediate upstream cross section of the bridge for the existing and proposed bridge pier for various river station and channel bottom width. The table also compares water surface elevation for both the channel scenarios (with and without ice jam). In the case of the channel without ice jam, the maximum difference in water surface elevation after the pier encasement was 0.04 ft attained for the river station Blair Road (93506.92). The same river station produced the maximum difference in water surface elevation of 0.03 ft for the channel with ice jam. The Figure 4-2 shows the plot between water surface elevation and flow at different stations. It showed no significant difference in headwater elevation between encased and non-encased pier condition. However, the difference in water surface elevation for the channel with a smaller bottom width (134 ft and 147 ft) was higher compared to channel with a bigger bottom width (251 ft and 231 ft).

Conclusions

The concept of pier encasement was successfully completed on the Grand River, NE Ohio. The study provided the necessary result to conclude that the rise in water surface elevation due to pier encasement was the function of channel bottom width. The smaller channel width resulted in an increase in headwater elevation. In addition, it was concluded that ice jam would not create an additional increase in water surface elevation particularly due to pier encasement. In overall, this application in the real world application further confirms the findings derived in chapter 2 and chapter 3 using generic channel section.

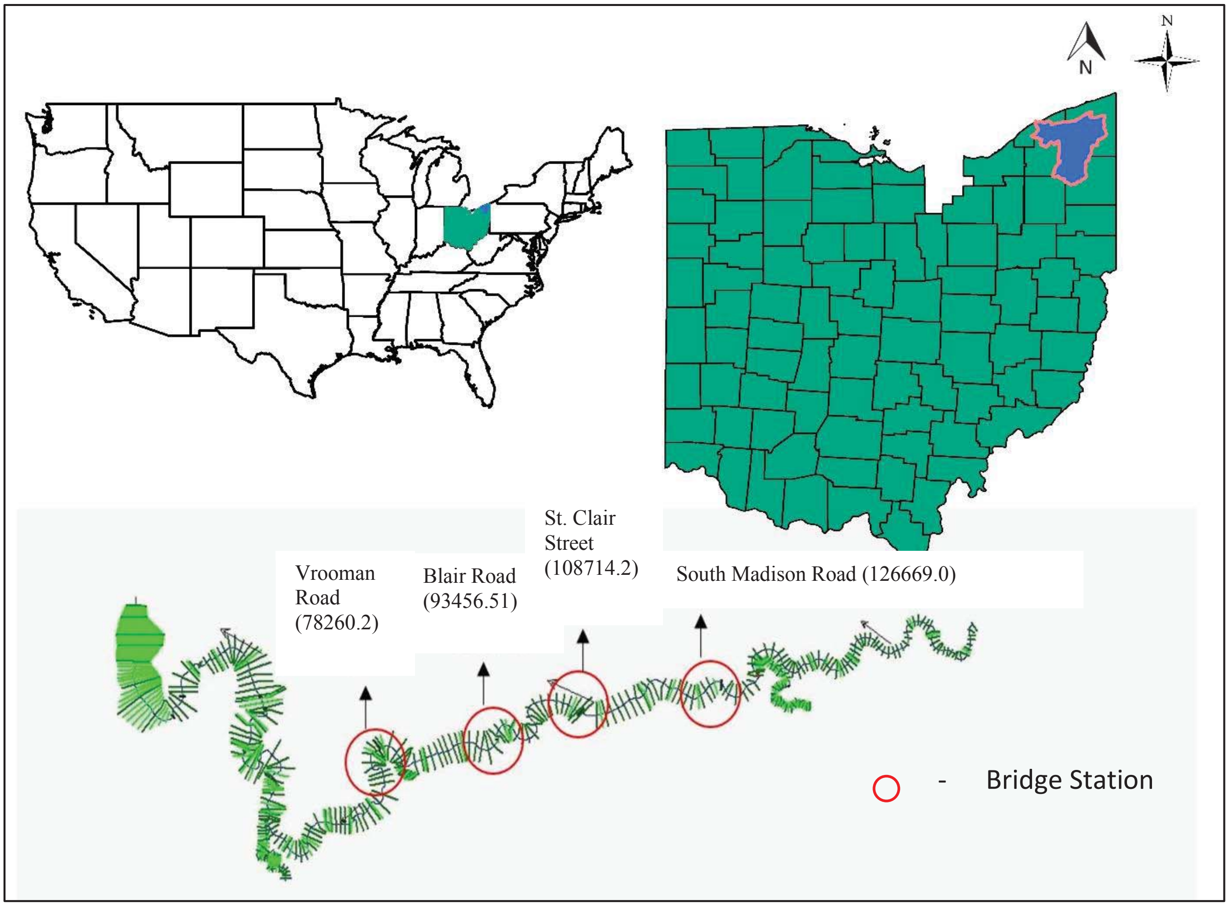

Figure 4-1: Hydraulic model of Grand River in HEC-RAS with bridge station number.

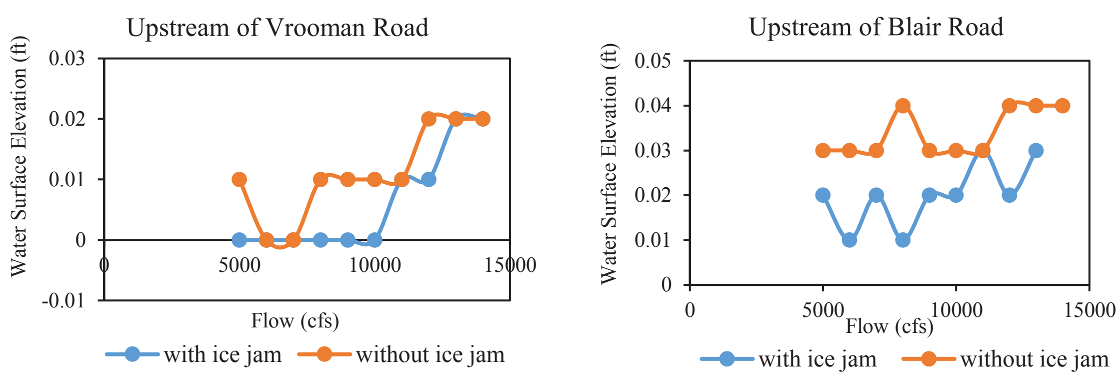

Figure 4-2: The difference in water surface elevation at bridge upstream before and after pier encasement for various bridge stations.

Table 4-1: The difference in water surface elevation before and after the pier encasement at bridge upstream

Channel Bottom Width (ft)	River Station	Flow	Water Surface Elevation without ice jam		Difference (ft)	Water Surface Elevation with ice jam		Difference (ft)
			Existing WSE (ft)	Proposed WSE (ft)		Existing WSE (ft)	Proposed WSE (ft)	
134	78320.81	6638.78	631.41	631.42	0.01	633.74	633.74	0
		9263.01	633	633.01	0.01	634.78	634.78	0
		10639.35	633.66	633.69	0.03	635.38	635.4	0.02
		11709.84	634.12	634.14	0.02	635.82	635.83	0.01
		13282.80	634.78	634.80	0.02	636.51	636.53	0.02
251	126736.9	6336.01	679.91	679.92	0.01	685.02	685.02	0
		8840.55	681.44	681.44	0	686.65	686.65	0
		10154.13	682.15	682.16	0.01	687.55	687.55	0
		11175.8	682.68	682.68	0	688.41	688.41	0
		12677.02	683.41	683.42	0.01	689.88	689.87	-0.01
213	108759	6336.01	662.26	662.26	0	664.34	664.34	0
		8840.55	664.34	664.34	0	666.52	666.52	0
		10154.13	665.32	665.32	0	667.52	667.52	0
		11175.8	666.02	666.02	0	668.22	668.22	0
		12677.02	666.98	666.98	0	669.2	669.2	0
147	93506.92	6336.01	645.65	645.68	0.03	647.74	647.75	0.01
		8840.55	647.34	647.37	0.03	649.43	649.45	0.02
		10154.13	648.06	648.09	0.03	650.17	650.19	0.02
		11175.8	648.56	648.6	0.04	650.7	650.72	0.02
		12677.02	649.25	649.28	0.03	651.42	651.45	0.03

References:

Lamichhane, Niraj. Prediction of Travel Time and Development of Flood Inundation Maps for Flood Warning System Including Ice Jam Scenario. A Case Study of the Grand River, Ohio. Diss. Youngstown State University, 2016.

Lamichhane, Niraj, and Suresh Sharma. "Development of Flood Warning System and Flood Inundation Mapping Using Field Survey and LiDAR Data for the Grand River near the City of Painesville, Ohio." Hydrology 4.2 (2017): 24.

Chapter 5. Conclusions and Recommendations

The Federal Emergency Management Administration (FEMA) defines the floodway boundaries under National Flood Insurance Program (NFIP) Zone AE. The developmental work within this floodway implies certain restriction, which is regulated by FEMA. In order to avoid the risk of flood, the developmental work within this floodplain should be minimized. FEMA denies any development work, which produces a surcharge of greater than 1.0 ft. The allowable discharge varies from State to State but in no case, it can cross the FEMA limit of 1 ft.

Bridges often cause a sudden change in water depth and flow directions. Moreover, with encasement of the pier during the process of bridge repair and rehabilitation, the analysis and calculation of water surface elevation at bridge vicinity become even more unpredictable. Therefore, this study conducted a parametric study and documented the effect of pile pier encasement on headwater elevation at the vicinity of the bridge by developing HEC-RAS model.

The hydraulic model was setup for various generic channel configuration and each channel configuration was run for two cases of encased and non-encased pier conditions. Bridge with a number of piers (2 & 3) and channel slope (0.3%, 0.5%, 0.7% and 1.0%) were developed and analyzed on the generic channel width varying from 20 ft to 180 ft kept at the interval of 20 ft. It was established from the analysis that increase in headwater elevation was a function of the width of the pier, flow volume, channel slope and bottom width.

The pier encasement results in an increase in pier width, which constricts the channel and increases the water surface elevation at bridge upstream. The channels with a steeper slope (0.7% and 1.0%) showed a greater rise in water surface elevation relative to flatter slopes. Moreover, the channel with a smaller width (20 ft, 40 ft, and 60 ft) showed greater rise in water surface elevation compared to wider channels (160 ft, 180 ft). In addition, flow also had a considerable effect on water surface elevation and it increased with the increase in flow.

Furthermore, the study of pier encasement effect on headwater elevation due to winter ice cover and ice jam was accomplished. The analysis was carried out in the same generic model with ice jam data. The rise in water surface elevation was computed using HEC-RAS for both encased and non-encased condition at bridge upstream. In this case, the rise in water surface elevation was comparatively less. The rise was observed only for smaller channel bottom (20 ft) with the steeper slopes (1.0% and 0.7%). For the wider channel, even the steeper slopes did not have a significant effect.

Finally, the application of the bridge pier encasement and its effect on headwater elevation at bridge upstream was analyzed for bridges located at Grand River, NE Ohio. As anticipated, the headwater elevation at the bridge upstream after the bridge pier encasement increased for the channel with smaller bottom width. On the other hand, the wider channel showed no changes in headwater elevation. Therefore, during pier encasement in bridges located at smaller river channel, it is essential to consider the rise is water surface elevation.